Cell cycle progression dictates the requirement for BCL2 in natural killer cell survival

Charlotte Viant,[1] Sophie Guia,[1] Robert J. Hennessy,[2,3] Jai Rautela,[2,3] Kim Pham,[2,3] Claire Bernat,[1] Wilford Goh,[2,3] Yuhao Jiao,[2,3,4] Rebecca Delconte,[2,3] Michael Roger,[1] Vanina Simon,[1] Fernando Souza-Fonseca-Guimaraes,[2,3] Stephanie Grabow,[2,3] Gabrielle T. Belz,[2,3] Benjamin T. Kile,[2,3] Andreas Strasser,[2,3] Daniel Gray,[2,3] Phillip D. Hodgkin,[2,3] Bruce Beutler,[5] Eric Vivier,[1,6] Sophie Ugolini,[1]* and Nicholas D. Huntington[2,3]*

[1]Centre d'Immunologie de Marseille-Luminy (CIML), Aix-Marseille Université, Centre National de la Recherche Scientifique (CNRS), Institut National de la Santé et de la Recherche Médicale (INSERM), 13288 Marseille, France
[2]The Walter and Eliza Hall Institute of Medical Research, Parkville, Victoria 3052, Australia
[3]Department of Medical Biology, University of Melbourne, Victoria 3010, Australia
[4]School of Medicine, Tsinghua University, Beijing 100084, China
[5]Center for the Genetics of Host Defense, University of Texas Southwestern Medical Center, Dallas, TX 75390
[6]Service Immunologie, Hôpital de la Conception, Assistance Publique Hôpitaux de Marseille (APHM), 13288 Marseille, France

Natural killer (NK) cells are innate lymphoid cells with antitumor functions. Using an *N*–ethyl–*N*–nitrosourea (ENU)–induced mutagenesis screen in mice, we identified a strain with an NK cell deficiency caused by a hypomorphic mutation in the *Bcl2* (*B cell lymphoma 2*) gene. Analysis of these mice and the conditional deletion of *Bcl2* in NK cells revealed a nonredundant intrinsic requirement for BCL2 in NK cell survival. In these mice, NK cells in cycle were protected against apoptosis, and NK cell counts were restored in inflammatory conditions, suggesting a redundant role for BCL2 in proliferating NK cells. Consistent with this, cycling NK cells expressed higher MCL1 (myeloid cell leukemia 1) levels in both control and BCL2–null mice. Finally, we showed that deletion of BIM restored survival in BCL2–deficient but not MCL1–deficient NK cells. Overall, these data demonstrate an essential role for the binding of BCL2 to BIM in the survival of noncycling NK cells. They also favor a model in which MCL1 is the dominant survival protein in proliferating NK cells.

INTRODUCTION

NK cells are innate lymphoid cells (ILCs) with cytotoxic and regulatory capacities. They develop in the BM and become dependent on the pleiotropic cytokine IL-15 shortly after committing to the NK cell lineage (Huntington et al., 2007b,c; Huntington, 2014). Mature NK cells can be identified in peripheral tissues by the coexpression of NKp46 (encoded by *Ncr1*) and high levels of IL-2Rβ (CD122), which forms IL-15 signaling heterodimer complexes with the gamma common cytokine receptor chain IL-2Rγ (CD132; γ$_C$) to permit NK cell responsiveness to IL-15. IL-15 induces several biological outcomes in NK cells that vary depending on the IL-15 concentration. In vivo, IL-15 is bound to and trans-presented by the IL-15Rα chain that is either present on the surface of IL-15/IL-15Rα–expressing cells or as cleaved soluble complexes (Cooper et al., 2002; Dubois et al., 2002; Koka et al., 2003; Burkett et al., 2004; Sandau et al., 2004; Mortier et al., 2008; Bergamaschi et al., 2012). The

steady-state levels of trans–presented IL-15 are thought to be low, maintaining NK cell survival while driving a minor fraction of NK cells into division. This is supported by the finding that only a small proportion of mature NK cells incorporated BrdU within a 2-wk pulse (Huntington et al., 2007b) and express Ki67 at steady-state (Jaeger et al., 2012) and by the failure of NK cells to undergo homeostatic proliferation when transferred into lymphoid-sufficient mice or even mice that specifically lack NK cells (Delconte et al., 2016b). However, experimentally, NK cells can be induced to proliferate after injection of IL-15R agonists (i.e., complexes formed by IL-15 and IL-15Rα-Fc or complexes formed by IL-2 and the anti–IL-2 monoclonal antibody S4B6) and are able to proliferate extensively in vitro for several weeks when given saturating amounts of IL-15 (Boyman et al., 2006; Rubinstein et al., 2006; Delconte et al., 2016b). Accessory immune cells, such as dendritic cells, also produce IL-15, leading to NK cell activation after pathogen recognition. For instance, Toll-like receptor 3 and 4 stimulation of dendritic cells results in IL-15Rα and IL-15 up-regulation and primes NK cell activity via their

IL-15Rβ/γ complexes, leading to optimal antiviral immunity (Lucas et al., 2007, 2010). IL-15 up-regulation in this scenario does not result in a major expansion of NK cells but leads to NK cell activation and synergizes with other cytokines, such as IL-12 and IL-18, to drive maximal effector function.

IL-15 binding to IL-15Rγ/β on NK cells results in the rapid phosphorylation of the receptor proximal JAK1 and JAK3 and the recruitment and phosphorylation of STAT5. Phospho-STAT5 homodimers then translocate to the nucleus, where they bind and activate STAT5-responsive genes (Soldaini et al., 2000; Rybner-Barnier et al., 2006). Deletion of IL-15 in vivo blocks NK cell development in mice, and NK cells fail to survive when adoptively transferred into $IL15^{-/-}$ mice. This indicates that IL-15 is essential for NK cell survival in vivo (Cooper et al., 2002; Dubois et al., 2002; Koka et al., 2003; Burkett et al., 2004; Sandau et al., 2004; Huntington et al., 2007a). IL-15 has long been known to promote NK cell survival, and several apoptosis inhibitory mechanisms have been uncovered. For example, IL-15 was shown to increase the expression of antiapoptotic proteins belonging to the BCL2 (B cell lymphoma 2) family, including BCL2, BCL-XL (encoded by $Bcl2l1$) and MCL1 (myeloid cell leukemia 1; Armant et al., 1995; Jiang et al., 1996; Ranson et al., 2003; Huntington et al., 2007c, 2009; Zheng et al., 2008; Hodge et al., 2009). We recently expanded on these data by showing that STAT5 directly drives $Mcl1$ expression by binding its 3′ UTR (Sathe et al., 2014). We demonstrated that when $Mcl1$ was deleted specifically in NK cells using $Ncr1^{iCre}$ knock-in mice, NKp46$^+$ NK cells and ILC1 were missing from all primary and secondary lymphoid organs. This demonstrates the essential role for MCL1 in regulating NK cell survival (Huntington et al., 2007a; Sathe et al., 2014). In the same study, we found that $Bcl2l1^{-/-}$ (BCLXL-deficient) mice had normal NK cell development, indicating the redundant role for this protein in the IL-15–dependent antiapoptotic pathway in NK cells. Although BCL2 had originally been shown to increase in NK cells in response to IL-15, we failed to detect any alteration in BCL2 levels after IL-15 withdrawal from NK cells, whereas MCL1 levels decreased dramatically corresponding with impaired NK cell survival (Huntington et al., 2007a). These data demonstrate an essential role for MCL1 in NK cell survival and questioned the role of BCL2.

RESULTS

Characterization of what else (WE) mice and identification of the causative mutation in Bcl2

NK cells contribute to the early antiviral response and tumor immune surveillance in part by sensing cells that have down-regulated MHC-I expression. To identify regulators of NK cell development and cytotoxicity, we devised an in vivo screening test in which we assayed the killing of MHC-I⁻ splenocytes, which is NK cell–dependent, in mice mutated by N-ethyl-N-nitrosourea (ENU). We uncovered several third–generation progeny with poor cytotoxicity against MHC-I⁻ cells in a pedigree called ENU-148 (Fig. 1 A). This

phenotype, named WE, was accompanied by progressive hair hypopigmentation (Fig. 1 B). Subsequent experiments revealed that the in vivo deficiency in cytotoxicity was associated with reduced numbers of NK cells in these mice (Fig. 1 C). In the ENU-148 pedigree, the immune and pigmentation defects were linked (Fig. 1 C), suggesting that a single autosomal-recessive mutation was responsible for the two phenotypes. To identify the causative mutation, DNA from a single WE mouse was subjected to whole-exome sequencing. DNA from six unrelated mice originating from other pedigrees generated in our ENU mutagenesis program was also sequenced. Only seven nonsense or missense homozygous mutations were selectively present in the WE mutant mouse. To identify the mutation responsible for the WE phenotype, we sequenced these seven genes in six other animals from the ENU-148 colony that did or did not exhibit the WE phenotype. Among these seven mutations, a homozygous mutation in $Bcl2$ (A1463G) was found to be the only one associated with the WE phenotype (Table 1 and Fig. 1 D). In accordance with the fact that a mutation in $Bcl2$ is responsible for the WE phenotype, the NK cell deficiency observed in $Bcl2^{WE/WE}$ mice was associated with a pan–lymphocytopenia also affecting CD4, CD8 T cells and B cells (Fig. 1 E) and abnormally small spleens (Fig. 1 F), as described earlier in $Bcl2$-deficient mice (Veis et al., 1993; Nakayama et al., 1994; Bouillet et al., 2001). In contrast, the myeloid compartment was normal (Fig. 1 G). Interestingly, when we compared the proportions of lymphocyte subsets in the spleens of $Bcl2^{WE/WE}$ mice, we observed that the T and B cells were unaffected compared with control mice whereas NK cells were significantly reduced (Fig. 1 H and not depicted), and we thus focused on dissecting the mechanisms by which mutation in $Bcl2$ was impacting NK cell homeostasis.

The mutation in WE mice caused a Y18C replacement in the BH4 domain of the BCL2 protein (Fig. 2 A). The expression of the $Bcl2$ mRNA in $Bcl2^{WE/WE}$ mice was comparable to $Bcl2^{+/+}$ controls (Fig. 2 B). In contrast, we could not detect the BCL2 protein by Western blotting (Fig. 2 C) and detected only a very low level of BCL2 by intracellular flow cytometry in $Bcl2^{WE/WE}$ mice (Fig. 2 D), although the antibodies used recognize epitopes outside the BH4 domain. Thus, BCL2 expression was drastically reduced in $Bcl2^{WE/WE}$ mice, resulting in a major NK cell deficiency, pan–lymphopenia, and hair hypopigmentation. On the basis of these data, and in the absence of severe pathologies (polycystic kidney and distorted small intestine) observed in $Bcl2^{-/-}$ mice (Veis et al., 1993; Nakayama et al., 1994; Bouillet et al., 2001), we concluded that the WE phenotype was caused by a hypomorphic mutation in the $Bcl2$ gene.

Preferential loss of mature NK cells in Bcl2^WE/WE mice

To further dissect the loss of peripheral NK cells in $Bcl2^{WE/WE}$ mice, we next analyzed NK cell maturation in the BM and spleen. The numbers of BM-resident NK cells were significantly reduced in $Bcl2^{WE/WE}$ mice (Fig. 3 A), and this mani-
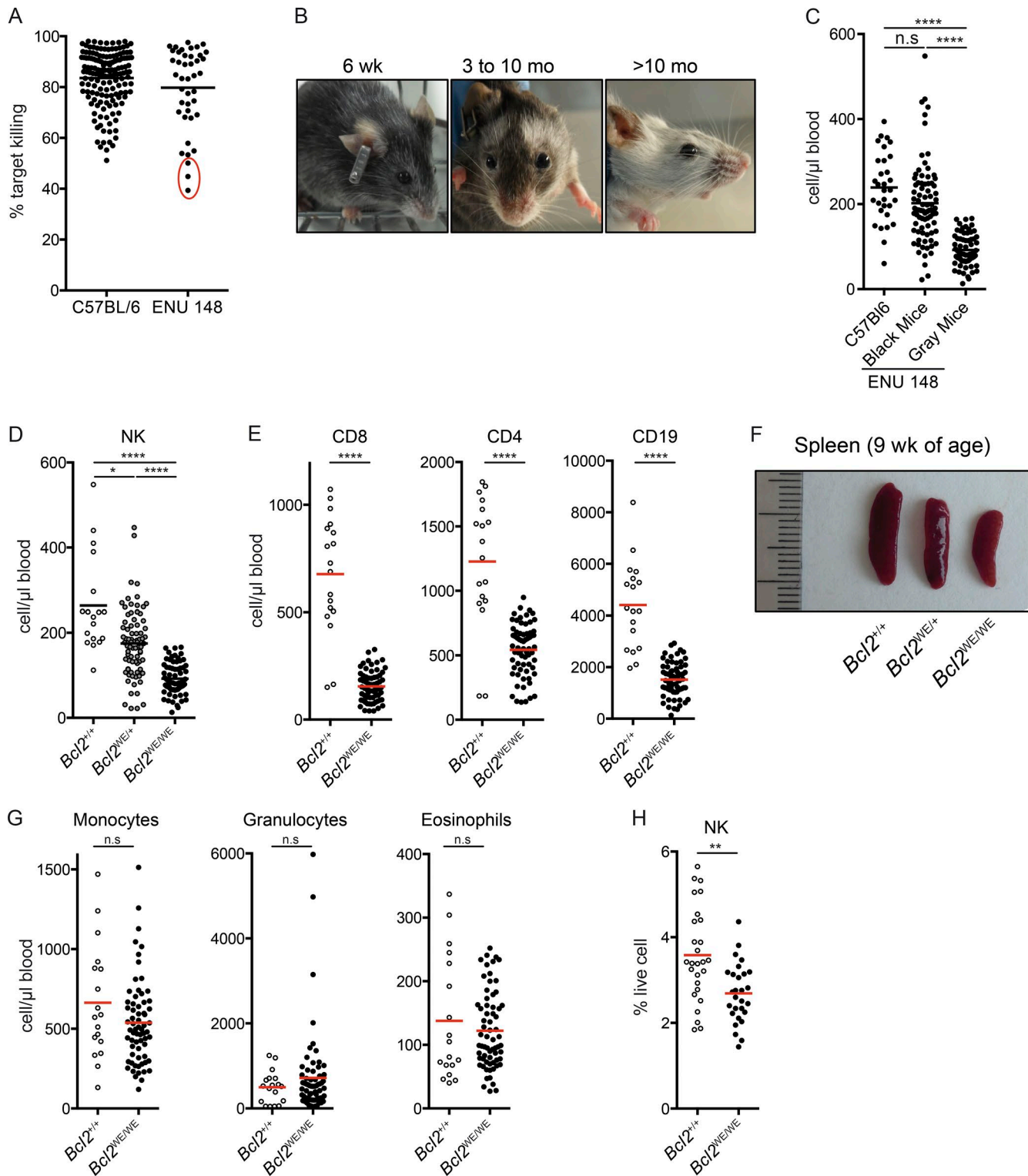
Figure 1. **Analysis of the *WE* mutant mouse phenotype and identification of the causative mutation.** (A) Selection of the ENU-148 pedigree using a functional screen based on an in vivo NK cell–killing assay. Splenocytes from WT and *b2m*-deficient (*b2m*$^{-/-}$) mice were isolated, stained with two different concentrations of the fluorescent dye CFSE, and injected i.v. into the indicated recipient mice (C57BL/6 control mice or G3 animals from pedigree ENU-148). 2 d after transfer, the relative frequency of the CFSE^{high} and CFSE^{low} populations present in the blood of recipient mice was assessed by flow cytometry, and the percentages of *b2m*$^{-/-}$ cell killing were calculated. Three G3 mice with a defect in NK cell–mediated target cell killing were selected (red circle) and

fested in a significant reduction in the number of all NK cells in maturation subsets (Fig. 3 B). Similarly, the $Bcl2^{WE/WE}$ mice presented with a significant reduction in splenic NK cell subsets (Fig. 3, C and D). In addition, there was a skewing toward a greater fraction of immature NK cells in $Bcl2^{WE/WE}$ mice, as $Bcl2^{WE/WE}$ mice contained significantly fewer CD43$^+$ NK cells compared with control animals (Fig. 3 D).

Cell-intrinsic requirement for *Bcl2* in NK cell development

We then analyzed whether the block in NK cell development was cell intrinsic by generating mixed-BM chimeras. When equal numbers of congenic CD45.1 and CD45.2 $Bcl2^{+/+}$ progenitors were transplanted into irradiated recipients, both progenitor populations contributed similarly to the resulting NK cell pool (Fig. 4 A). In contrast, when CD45.2 $Bcl2^{WE/WE}$ progenitors were transplanted in competition with equal numbers of CD45.1 $Bcl2^{+/+}$ progenitors, all NK cells from recipient mice were derived from the $Bcl-2^{+/+}$ progenitors. These data revealed a cell-intrinsic requirement for BCL2 for NK cell development and/or maintenance (Fig. 4 A). To test whether $Bcl2$ was required in NK cells themselves or at an earlier progenitor stage, we conditionally deleted $Bcl2$ in NKp46$^+$ NK cells by intercrossing the $Bcl2^{fl/fl}$ strain (Thorp et al., 2009) with the $Ncr1^{iCre}$ strain, in which Cre-mediated deletion of floxed genes occurs at the immature stage of NK cell development (Narni-Mancinelli et al., 2011). Consistent with an intrinsic role for $Bcl2$ in NK cell survival in vivo, $Ncr1^{iCre/+}Bcl2^{fl/fl}$ mice presented with a significant reduction in peripheral NK cells (Fig. 4 B). NK cell lymphopenia in $Ncr1^{iCre/+}Bcl2^{fl/fl}$ mice was greater than that observed in $Bcl2^{WE/WE}$ mice, both in terms of fold reduction compared with littermate controls and in absolute cell numbers (Fig. 4 B). The defect in NK cell development in $Ncr1^{iCre/+}Bcl2^{fl/fl}$ mice was accompanied by reduction in NK cells counts for both immature and mature subsets, with a more dramatic reduction in mature pools compared with that seen in littermate controls (Fig. 4 C). As a result, NK cells in the periphery of $Ncr1^{iCre/+}Bcl2^{fl/fl}$ mice were immature in phenotype, and these mice harbor a lower proportion of CD43$^+$ NK cells (Fig. 4 C). $Ncr1^{iCre/+}Bcl2^{fl/fl}$ mice were healthy, and as expected, unlike $Bcl2^{WE/WE}$ mice, they did not develop progressive hair hypopigmentation or pan-lymphopenia (Fig. 4 D). Collectively, these results show that BCL2 is required in a cell-intrinsic manner for normal NK cell homeostasis.

Despite their normal responsiveness, impaired NK cell survival in *Bcl2*-deficient mice culminates in a poor antitumor response in vivo

We next investigated whether NK cell effector functions were compromised in $Bcl2$-deficient mice. NK cell responsiveness was tested in vitro after NK1.1 receptor or cytokine (IL-12/IL-18) stimulation. The NK cells from $Bcl2^{WE/WE}$ mice were as responsive as NK cells from WT animals (Fig. 5 A), demonstrating that BCL2 is not required for NK cell activation in vitro. We then looked at antitumor responses. NK cells from $Bcl2^{WE/WE}$ mice were cultured with IL-2 to obtained leukocyte-activated killer (LAK) cells. We then analyzed the activation of these cells against YAC-1 tumor cell line (Fig. 5 B). Similarly, the activation of $Bcl2^{WE/WE}$ LAK cells was unchanged compared with that observed in control LAK cells. We next challenged $Ncr1^{iCre/+}Bcl2^{fl/fl}$ and $Ncr1^{iCre/+}Bcl2^{+/+}$ mice with a breast cancer line (EO771-LMB) that preferentially metastasizes to the lung when injected i.v. $Ncr1^{iCre/+}Bcl2^{fl/fl}$ mice were unable to clear lung metastasis as efficiently as $Ncr1^{iCre/+}Bcl2^{+/+}$, mice suggesting that the severe NK cell lymphopenia observed in this model was responsible for the impaired antitumor response in vivo (Fig. 5 C). Collectively, these data indicate that BCL2 is required for normal NK cell development but dispensable for NK cell activation.

Impaired NK cell survival in *Bcl2*–deficient mice is restored in inflammatory conditions

Next, we analyzed the rate of NK cell apoptosis in $Bcl2^{WE/WE}$ mice to verify whether enhanced apoptosis was the cause of the NK cell lymphopenia. Indeed, $Bcl2^{WE/WE}$ NK cells were more sensitive to growth factor withdrawal, with ∼80% of peripheral $Bcl2^{WE/WE}$ NK cells undergoing apoptosis compared with ∼20% of $Bcl2^{+/+}$ NK cells after 4 h in culture medium (Fig. 6 A). We then tested whether the survival of BCL2-deficient NK cells could be boosted in inflammatory conditions. $Bcl2^{WE/WE}$ mice were challenged with mouse cytomegalovirus (MCMV), which is known to induce potent NK cell expansion. Interestingly, NK cells in $Bcl2$-deficient mice expanded more than those in WT controls. This resulted in a NK cell pool similar to that of control mice 7 d after MCMV infection (Fig. 6 B). These data suggest that the requirement for BCL2 in NK cell survival was different at steady-state versus inflammatory conditions. As NK cells undergo substantial proliferation upon MCMV infection, we examined whether IL-15 receptor stimulation, which also induces pro-

---

crossed to WT animals to generate a colony of mutant mice. An autosomal-recessive transmission of the mutation was observed, and the phenotype of affected animals was called *WE*. (B) In the ENU-148 colony, some mice showed progressive hair hypopigmentation. The pictures show a typical example of this phenotype for mice aged between 6 wk and >10 mo, as indicated. (C) NK cell counts in the blood of control (C57BL/6J) mice and mice from the pedigree ENU-148 presenting or not with hair hypopigmentation (gray and black, respectively). Each dot represents the results obtained for one mouse ($n = 31$–82, Kruskal–Wallis statistical test). (D) ENU-148 mice were segregated depending on their $Bcl2$ genotype, and the NK cell counts in peripheral blood were measured. Each dot represents the results obtained from an individual mouse ($n = 18$–79, Kruskal–Wallis statistical test). (E) Enumeration of CD4$^+$, CD8$^+$ T cells and B cells in the blood of $Bcl2^{+/+}$ and $Bcl2^{WE/WE}$ mice ($n = 18$–67, Mann–Whitney statistical test). (F) Comparison of the size of the spleens from 9-wk-old $Bcl2^{+/+}$, $Bcl2^{WE/+}$, and $Bcl2^{WE/WE}$ mice. (G) Enumeration of monocytes, granulocytes, and eosinophils in the blood of $Bcl2^{+/+}$ and $Bcl2^{WE/WE}$ mice ($n = 18$–67, Mann–Whitney statistical test). (H) Percentage of NK cells in the spleens of $Bcl2^{+/+}$ and $Bcl2^{WE/WE}$ mice ($n = 28$, Mann–Whitney statistical test). Each dot corresponds to the data obtained from an individual mouse. Horizontal lines indicate the mean. *, P < 0.05; **, P < 0.01; and ****, P < 0.0001.

A BCL2 protein

BH4 | BH3 | BH1 | BH2 | TM

Y18C point mutation

B

Fold change $Bcl2^{WE/WE}/Bcl2^{+/+}$

C

kD

$Bcl2^{+/+}$ $Bcl2^{WE/+}$ $Bcl2^{WE/WE}$

37 —
25 —
20 —

BCL2: 26 kD

50 —
37 —

ß-ACTIN: 43 kD
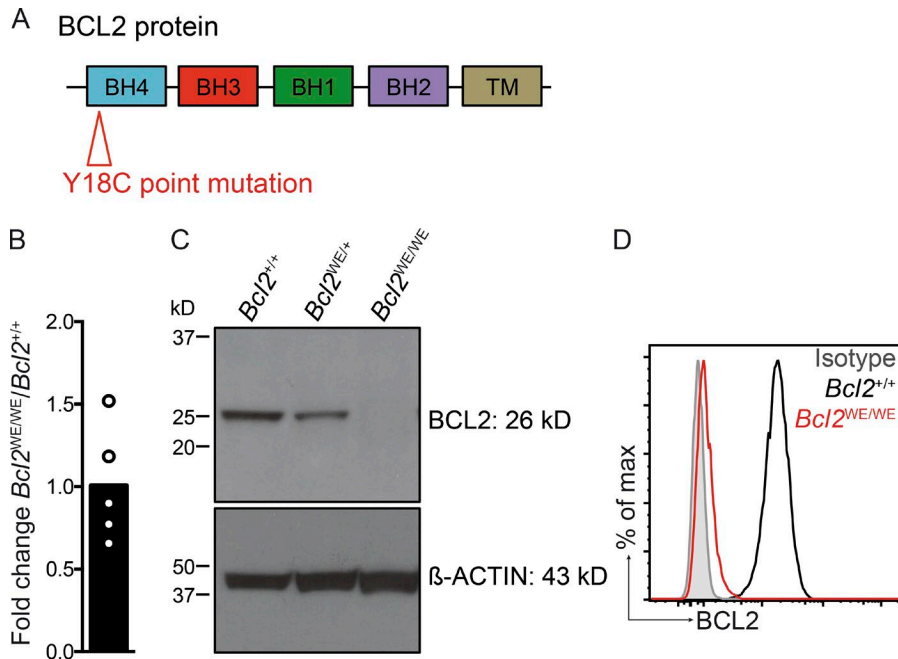
D

% of max

Isotype
$Bcl2^{+/+}$
$Bcl2^{WE/WE}$

BCL2

Figure 2. ***Bcl2* expression in *WE* splenocytes.** (A) Schematic representation of the BCL2 protein. The point mutation responsible for the *WE* phenotype induces a change of tyrosine to cysteine at amino acid position 18 in the BH4 domain of the BCL2 protein. (B) *Bcl2* mRNA expression was assessed by quantitative RT-PCR. The fold change in the expression of *Bcl2* transcripts in $Bcl2^{WE/WE}$ versus $Bcl2^{+/+}$ splenocytes is shown ($n = 5$). Each dot on the figure corresponds to the data obtained for a single experiment. (C) Analysis of BCL2 protein expression by immunoblotting in splenocytes from $Bcl2^{WE/WE}$, $Bcl2^{WE/+}$, and $Bcl2^{+/+}$ mice (representative of three independent experiments). Probing for β-ACTIN was used as a loading control. (D) BCL2 expression was analyzed by flow cytometry. Representative intracellular staining of BCL2 in splenic NK cells from $Bcl2^{WE/WE}$ and $Bcl2^{+/+}$ mice are shown (data shown are representative of three independent experiments).

found NK cell proliferation, could rescue the NK cell deficiency in BCL2-deficient mice. $Ncr1^{iCre/+}Bcl2^{+/+}$ and $Ncr1^{iCre/+}Bcl2^{fl/fl}$ mice were treated with the IL-15 receptor agonist IL-2 complexed with anti–IL-2 monoclonal antibody (clone S4B6) on days 0, 2, and 4, as we have previously shown that this results in a large expansion of NK cells by day 7 (Narni-Mancinelli et al., 2012). We observed a ~20-fold expansion of $Ncr1^{iCre/+}Bcl2^{fl/fl}$ NK cells compared with a 10-fold expansion of $Ncr1^{iCre/+}Bcl2^{+/+}$ control NK cells after IL-2/S4B6 treatment (Fig. 6 C). The majority of these NK cells were cycling, as revealed by their expression of the cell proliferation marker Ki67 (Fig. 6 D). In contrast, no rescue or expansion of $Ncr1^{iCre/+}Mcl1^{fl/fl}$ NK cells was observed after

IL–2/S4B6 treatment (Fig. 6 C). This demonstrates a differential intrinsic requirement for BCL2 versus MCL1 in NK cell survival during proliferation. These results show that BCL2-deficient NK cells are abnormally prone to undergo apoptosis, resulting in a profound NK cell deficiency in BCL2-deficient mice. This defect can be at least partially rescued in inflammatory conditions, which promote extensive NK cell proliferation.

Bcl2 loss is intrinsically linked to an increase of proliferating NK cells

Surprisingly, we observed that without any stimulation, in steady-state conditions, a large proportion of NK cells

Table 1. Identification of a point mutation in the *Bcl2* gene on Chr1 as the causative mutation for the *WE* phenotype

Mouse ID number	Phenotype		Mutations						
			Arg2	*Bcl2*[a]	*Erbp4*	*Lama1*	*Naip2*	*Satb2*	*Slc15a2*
			chr12 :80248736	chr1 :108609405[a]	chr1 :68607208	chr17 :68102223	chr13 :1000931864	chr1 :56907005	chr16 :36772531
	Lymphopenia	Depigmentation	A → T	T → C[a]	G → A	G → A	A → T	G → A	A → G
9610	Yes	Yes	–	Yes[a]	Yes[a]	No[b]	No[b]	Yes[a]	–
9184	No	No	No[a]	No[a]	Yes[b]	Yes[b]	Yes[b]	No[a]	Yes[b]
9564	Yes	Yes	No[b]	Yes[a]	–	No[b]	No[b]	–	–
9611	Yes	Yes	–	Yes[a]	No[b]	No[b]	No[b]	–	Yes[a]
9559	Yes	Yes	Yes[a]	Yes[a]	No[b]	No[b]	No[b]	–	–
9607	Yes	Yes	No[b]	Yes[a]	–	–	No[b]	No[b]	Yes[a]

Whole-exome sequencing was performed on the DNA of one ENU-198 G5 mouse displaying the *WE* phenotype. All the mutations that were also found in six other mice from other pedigrees in our ENU mutagenesis program were excluded. The seven homozygous point mutations, which were selectively found in the *WE* mouse, are presented in this table. To identify the mutation responsible for the *WE* phenotype, we analyzed the presence of these mutations in other ENU-198 G5 animals displaying (for mice 9610, 9564, 9611, 9559, and 9607) or not displaying (9184) the *WE* phenotype (lymphopenia and hair hypopigmentation). The homozygous mutation in the *Bcl2* gene (A1463G) is the only one, which was strictly associated with the *WE* phenotype. The whole *Bcl2* gene was also sequenced in another *WE* mutant mouse. The A1463G mutation was the only mutation present in the *Bcl2* gene.
[a]Genotypes for the indicated genes and *WE* phenotype are consistent.
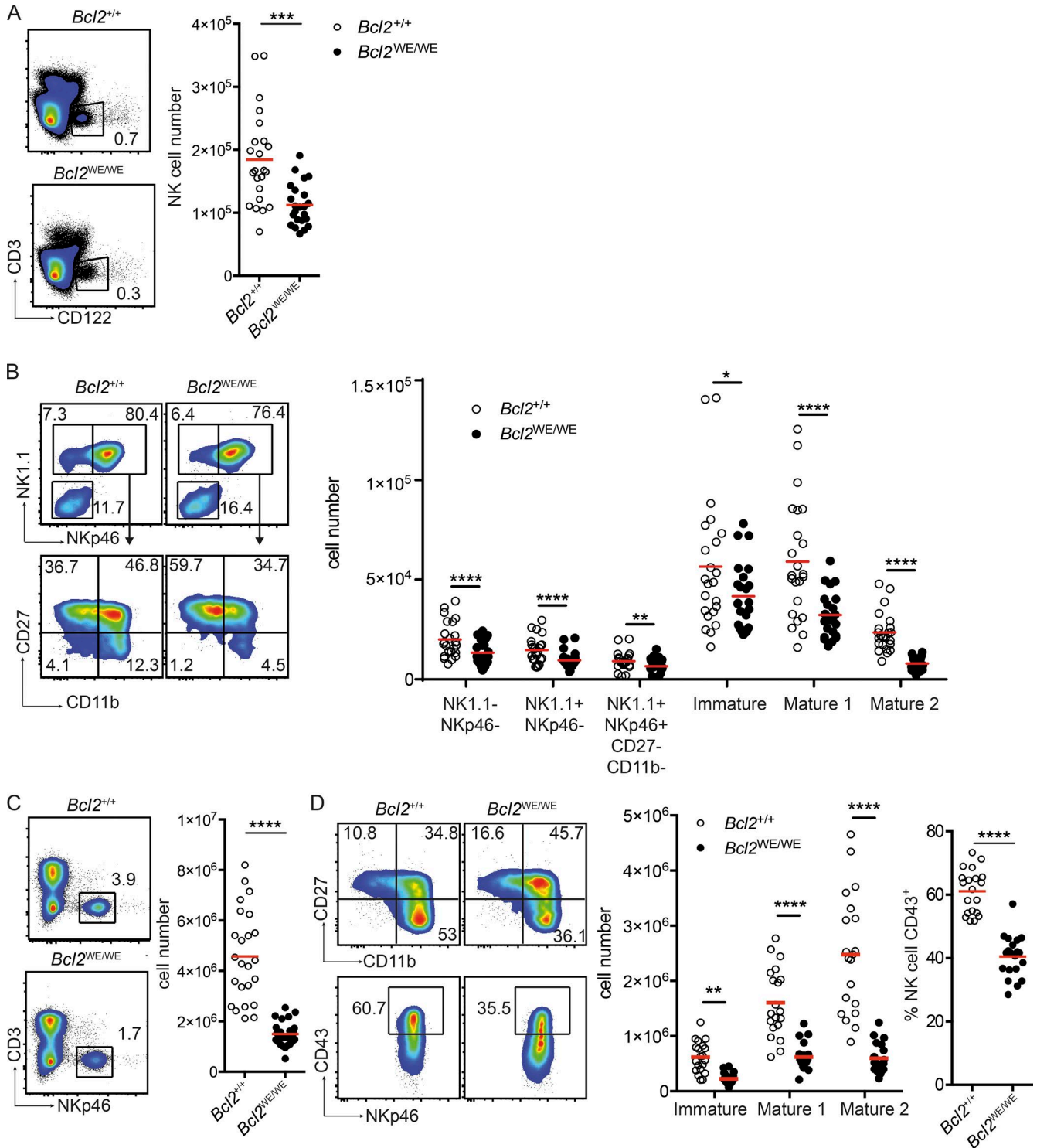[b]Genotypes for the indicated genes and *WE* phenotype are discordant.

Figure 3. **NK cells in the BM and the spleen of *WE* mice display an immature phenotype.** (A, left) Representative flow cytometric profiles of BM-derived NK cells (CD122⁺ CD3⁻) from *Bcl2⁺/⁺* and *Bcl2ᵂᴱ/ᵂᴱ* mice. (right) NK cell counts in the BM of *Bcl2⁺/⁺* and *Bcl2ᵂᴱ/ᵂᴱ* mice (n = 23, Mann–Whitney statistical test). (B, left) Representative flow cytometric profiles of BM NK cell maturation states from *Bcl2⁺/⁺* and *Bcl2ᵂᴱ/ᵂᴱ* mice: NK1.1⁻ NKp46⁻, NK1.1⁺ NKp46⁻, NK1.1⁺ NKp46⁺ CD27⁻ CD11b⁻, NK1.1⁺ NKp46⁺ CD27⁺ CD11b⁻ (immature), NK1.1⁺ NKp46⁺ CD27⁺ CD11b⁺ (mature 1), and NK1.1⁺ NKp46⁺ CD27⁻ CD11b⁺ (mature 2). (right) The relative cell counts of subsets of CD122⁺ CD3⁻ BM NK cells is shown based on their maturation states (n = 23, paired Student's *t* test). (C, left) Representative flow cytometric profiles of splenic NK cells (CD3⁻ NKp46⁺) from *Bcl2⁺/⁺* and *Bcl2ᵂᴱ/ᵂᴱ* mice. (right) NK cell counts in spleens from *Bcl2⁺/⁺* and *Bcl2ᵂᴱ/ᵂᴱ* mice (n = 25, Mann–Whitney statistical test). (D) Representative flow cytometric profiles (left) and relative frequency

were in cell cycle in both $Ncr1^{iCre/+}Bcl2^{fl/fl}$ and $Bcl2^{WE/WE}$ mice (Figs. 6 D and 7 A). The enhanced proliferative state of $Bcl2$-deficient NK cells was consistently observed at all stages of NK cell maturation (Fig. 7 B) and thus was not caused by the enhanced proportion of immature NK cells, which are known to cycle faster than mature NK cells (Huntington et al., 2007b). This phenotype could reflect a differential requirement for BCL2 through cell division or enhanced homeostatic proliferation in lymphopenic conditions. To resolve this question, we analyzed NK cell proliferation in $Ncr1^{iCre/+}Bcl2^{fl/fl}$ mice. In these animals, $Ncr1$-Cre–mediated deletion results in both BCL2$^+$ and BCL2$^-$ populations among NK1.1$^+$NKp46$^+$ NK cells (Fig. 7 C). This phenomenon is most likely caused by the long half–life (>20 h) of the BCL2 protein (Maurer et al., 2006). Thus, whereas all $Ncr1^{iCre/+}Bcl2^{fl/fl}$ NK1.1$^+$NKp46$^+$ NK cells express readily detectable levels of BCL2 by flow cytometry, we were still able to detect a small fraction of Cre-expressing (NK1.1$^+$NKp46$^+$) NK cells in $Ncr1^{iCre/+}Bcl2^{fl/fl}$ mice that maintained detectable BCL2 expression (Fig. 7 C). Electronically gating on NK cells based on BCL2 expression among the Cre-expressing $Ncr1^{iCre/+}Bcl2^{fl/fl}$ NK cells revealed that only the BCL2$^-$ NK cells displayed the hyperproliferative phenotype, whereas $Bcl2$ gene–deleted NK cells still expressing BCL2 protein resembled control NK cells in terms of Ki67 expression (Fig. 7 C). These data show that BCL2 loss in NK cells is intrinsically linked to an increased proliferative state.

NK cells in cell cycle are less dependent on BCL2 for their survival than quiescent NK cells

We next set out to address how the loss of BCL2 results in an increase in cycling NK cells. The fact that most of the remaining viable NK cells in $Bcl2^{WE/WE}$ and $Ncr1^{iCre/+}Bcl2^{fl/fl}$ mice were proliferating (Ki67$^+$; Fig. 7, A and B) suggested that BCL2 is either preferentially required for the survival of nondividing NK cells or that the absence of BCL2 drives NK cells into proliferation. To distinguish between these possibilities, we first performed in vitro experiments using a potent inhibitor of BCL2, ABT-199, which has shown success in clinical trials of chemotherapeutic drug treatment refractory chronic lymphocytic leukemia (CLL; Maurer et al., 2006) and was recently approved by the US Food and Drug Administration for treatment of CLL with 17p chromosomal deletion. To inhibit BCL2 in healthy BCL2-sufficient NK cells, we treated freshly isolated C57BL/6 splenic NK cells with various doses of ABT-199 in vitro in the presence of IL-15 and monitored Ki67 expression by flow cytometry after 20 h. Consistent with our

in vivo findings, ABT-199 treatment increased the Ki67$^+$ fraction of viable NK cells, with this reaching significance at a dose of >100 nM ABT-199 (Fig. 8 A). Importantly, when we enumerated the Ki67$^+$ and the Ki67$^-$ fractions of NK cells after ABT-199 treatment, we observed a drastic reduction of Ki67$^-$ NK cells, whereas the KI67$^+$ fraction was less sensitive to the cell loss induced by the BCL2 inhibitor (Fig. 6 A). These data suggest that BCL2 is required for optimal NK cell survival and that dividing NK cells are less dependent on BCL2 compared with quiescent NK cells. Consistent with this model, when we compared the total numbers of Ki67$^+$ splenic NK cells in the $Ncr1^{iCre/+}Bcl2^{fl/fl}$ and $Bcl2^{WE/WE}$ mice to their relevant control animals, we failed to observe any significant difference (Fig. 8 B). In contrast, the numbers of Ki67$^-$ NK cells were dramatically reduced in the two BCL2-deficient strains. The drastic reduction in NK cells after BCL2 loss was thus restricted to the Ki67$^-$ population both in vivo and in vitro. We next adopted an in vitro cell proliferation assay to gain further insight into how the loss of BCL2 function alters NK cell survival and proliferation (Hawkins et al., 2007; Marchingo et al., 2014). C57BL/6 splenic NK cells were cultured in cytostatic and saturating proliferative concentrations of IL-15 with and without ABT-199. When cultured with 10 ng/ml IL-15, close to 40% of NK cells survive without dividing for up to 170 h (Fig. 8 C). ABT-199 induced the rapid death of these cells, leading to a 99.9% reduction within 50 h of exposure. When cultured in 200 ng/ml IL-15, NK cells undergo an initial loss and then proliferate rapidly after 50 h (Fig. 8 D). Addition of ABT-199 leads to increased early loss of cells but had little effect on the rate of division observed after 50 h. This confirms a much weaker role for BCL2 in promoting survival once division is initiated. Cell trace violet (CTV) was used to analyze the successive rounds of cell division in the presence of increasing doses of ABT-199. CTV profiles of cells taken at 69.5 h (Fig. 8 E) illustrated that the number of cell divisions was not modified in the presence of the BCL2 inhibitor; this was also evident by identical mean division number over time plots (Fig. 8, C and D). However, the loss of cells in the undivided peak in the presence of 100 nM ABT-199 increased the ratio of divided to undivided cells in the culture as seen in Fig. 8 A.

These data strongly suggest that NK cells in cell cycle are less dependent on BCL2 than quiescent NK cells for their maintenance. Furthermore, these data support the conclusion that BCL2 is preferentially required for the survival of nonmitotic NK cells as opposed to the hypothesis that loss of BCL2 intrinsically drives NK cells into cell division.

of NK cell subsets (right) of splenic NK cells from $Bcl2^{+/+}$ and $Bcl2^{WE/WE}$ mice: NK1.1$^+$ NKp46$^+$ CD27$^+$ CD11b$^-$ (immature), NK1.1$^+$ NKp46$^+$ CD27$^+$ CD11b$^+$ (mature 1), NK1.1$^+$ NKp46$^+$ CD27$^-$ CD11b$^+$ (mature 2; n = 20, two-way ANOVA with Bonferroni correction statistical test), and CD43$^+$ expression (n = 20, Mann–Whitney statistical test). Each dot represents the data obtained from an individual mouse. Horizontal lines indicate the mean. *, P < 0.05; **, P < 0.01; ***, P < 0.001; and ****, P < 0.0001.
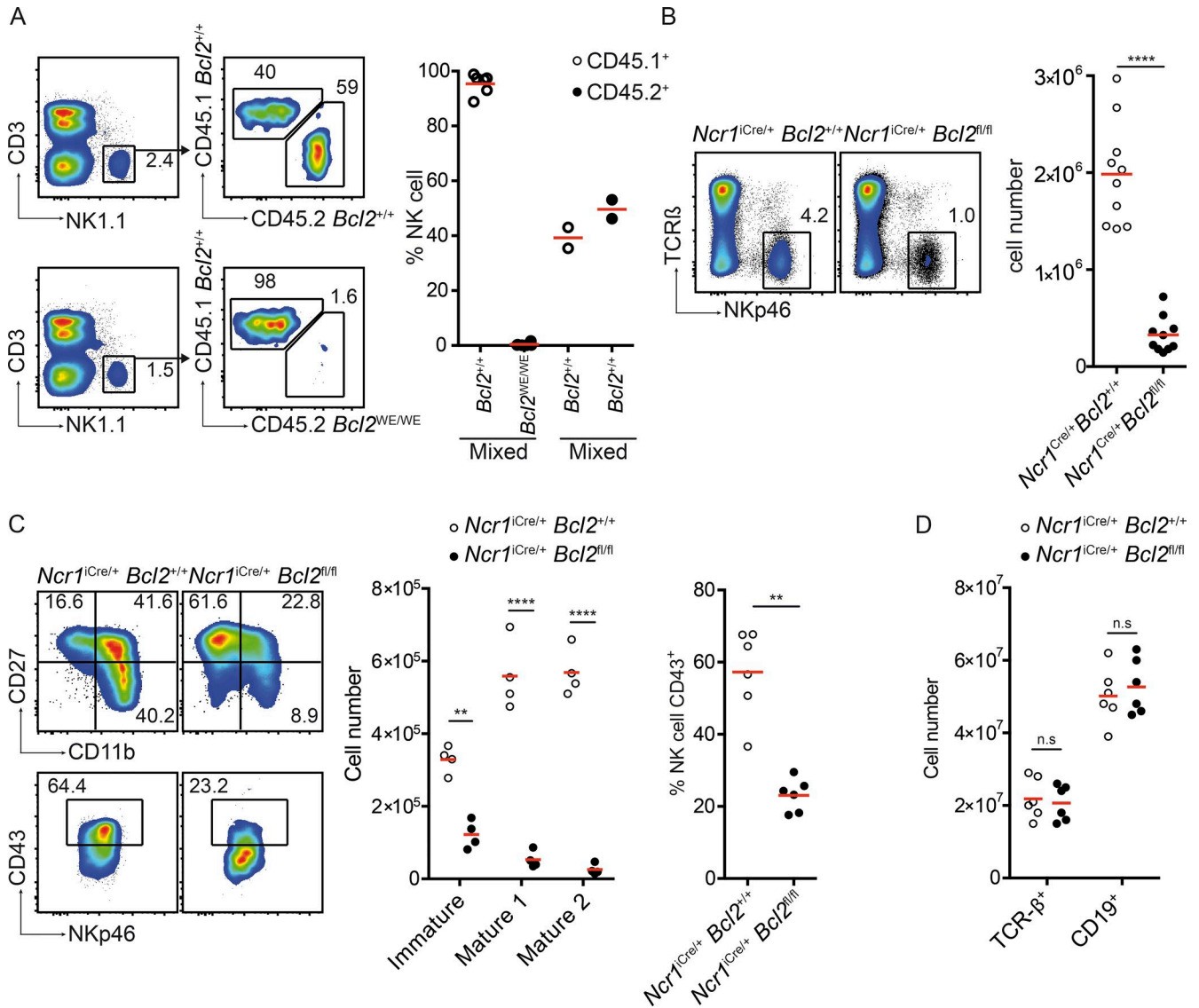
Figure 4. **A cell–intrinsic role of BCL2 in NK cell homeostasis.** (A) Mixed BM chimera experiments were performed. WT CD45.1^{+} BM cells were mixed at a 1:1 ratio with either CD45.2[+] *Bcl2*[WE/WE] or CD45.2[+] *Bcl2*^{+/+} BM cells and transferred into lethally irradiated WT CD45.1 recipient. Chimeric mice were analyzed 12 wk later. (left) Representative flow cytometric profiles of NK cell reconstitution in the spleens of chimeric *WT/Bcl2*^{+/+} (top) and *WT/Bcl2*[WE/WE] (bottom) mice stained with anti-CD45.1 and anti-CD45.2 mAbs. (right) The percentages of CD45.1[+] and CD45.2^{+} NK cells in the two groups of chimeras are shown. (B, left) Representative flow cytometric profiles of spleen NK cells (TCRβ[−] NKp46^{+}) from *Ncr1*[iCre/+]*Bcl2*^{+/+} and *Ncr1*[iCre/+]*Bcl2*^{fl/fl} mice. (right) NK cell counts in the spleens of *Ncr1*[iCre/+]*Bcl2*^{+/+} and *Ncr1*[iCre/+]*Bcl2*^{fl/fl} mice (*n* = 10, Mann–Whitney statistical test). (C) Representative flow cytometric analysis (left) and relative counts of NK cell subsets in the spleens of *Ncr1*[iCre/+]*Bcl2*^{+/+} and *Ncr1*[iCre/+]*Bcl2*^{fl/fl} mice were analyzed (middle): NK1.1^{+} NKp46^{+} CD27^{+} CD11b^{−} (immature), NK1.1^{+} NKp46^{+} CD27^{+} CD11b^{+} (mature 1), NK1.1^{+} NKp46^{+} CD27^{−} CD11b^{+} (mature 2; *n* = 4, two-way ANOVA with Bonferroni correction statistical test). CD43 expression on NK cells is also shown (right; *n* = 6, Mann-Whitney statistical test) of *Ncr1*[iCre/+]*Bcl2*^{+/+} and *Ncr1*[iCre/+]*Bcl2*^{fl/fl} mice. (D) T and B cell counts in the spleens of *Ncr1*[iCre/+]*Bcl2*^{+/+} and *Ncr1*[iCre/+]*Bcl2*^{fl/fl} mice (*n* = 6, two-way ANOVA with Bonferroni correction statistical test). Each dot corresponds to the data obtained from an individual mouse. Horizontal lines indicate the mean. **, P < 0.01; and ****, P < 0.0001.

Different dependency on BCL2 by distinct NK cell subsets is linked to variations in MCL1 levels

We previously demonstrated that *Ncr1*[iCre/+]*Mcl1*^{fl/fl} lacked all peripheral NK cell subsets and that IL-15 signaling directly regulated *Mcl1* transcription to protect NK cells from apoptosis (Sathe et al., 2014). Given that BCL2 and MCL1 appear to play nonredundant roles in NK cell survival in vivo and the fact that both prosurvival proteins bind the BH3-only protein BIM, a key mediator of NK cell apoptosis, we set out to investigate if MCL1 was altered in the absence of BCL2 in NK cells. MCL1 expression in *Ncr1*[iCre/+]*Bcl2*^{fl/fl} NK cells was clearly higher compared with NK cells from
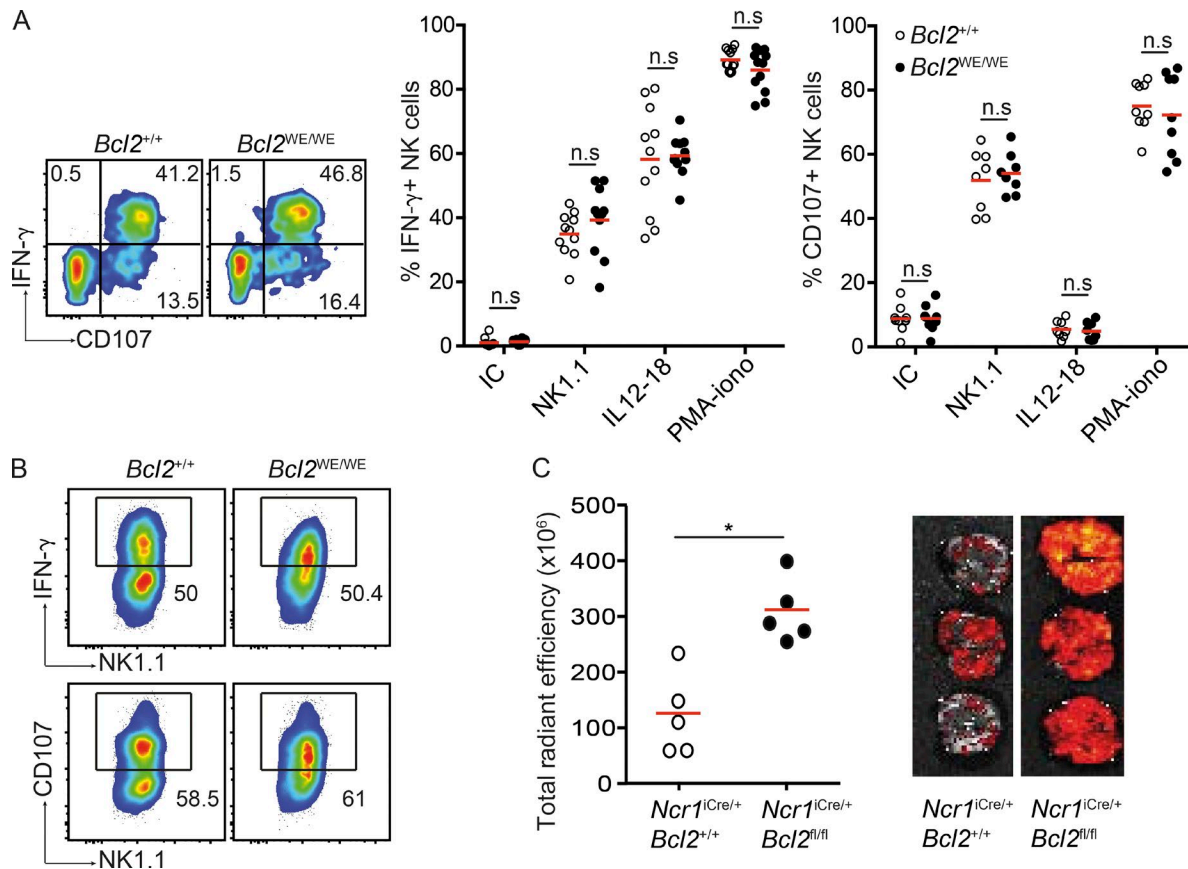
Figure 5. **NK cell responsiveness in *Bcl2*[WE/WE] mutant mice.** (A, left) Representative flow cytometric profiles of IFN-γ and CD107 expression in *Bcl2*^{+/+} or *Bcl2*[WE/WE] NK cells after 4 h of NK1.1 stimulation. (middle and right) Percentage of IFN-γ+ or CD107+ NK cells after 4 h of activation with an Ig isotype-matched control mAb (IC), anti-NK1.1 mAb, IL-12, and IL-18 or PMA plus ionomycin (PMA-iono; n = 8–11, two-way ANOVA with Bonferroni correction statistical test). Each dot corresponds to the data obtained from a single mouse. (B) Representative flow cytometric profiles of IFN-γ and CD107 expression in *Bcl2*^{+/+} or *Bcl2*[WE/WE] LAK cells, after 4 h of incubation with YAC-1 cells. Representative of four mice in two experiments. (C) *Ncr1*[iCre/+]*Bcl2*^{+/+} and *Ncr1*[iCre/+]*Bcl2*^{fl/fl} mice were injected i.v. with E0771-LMB mCherry+ breast cancer cells. Lung metastases were measured 14 d later by IVIS Spectrum in vivo imaging system (PerkinElmer) for mCherry fluorescence (vertical axis: total radiant efficiency [(p/s)/IW/cm²] × 1e⁶). P = 0.008, n = 5, Mann–Whitney statistical test. Horizontal lines indicate the mean. *, P < 0.05.

control *Ncr1*[iCre/+]*Bcl2*^{+/+} animals, and this was also the case for *Bcl2*[WE/WE] NK cells (Fig. 9 A). Given the skewed proportion of Ki67+ NK cells in *Ncr1*[iCre/+]*Bcl2*^{fl/fl} and *Bcl2*[WE/WE] mice, we subdivided NK cells from control (*Ncr1*[iCre/+]*Bcl2*^{+/+} or *Bcl2*^{+/+}) and BCL2 mutants (*Ncr1*[iCre/+]*Bcl2*^{fl/fl} or *Bcl2*[WE/WE]) mice based on Ki67 expression. This revealed that Ki67+ NK cells expressed higher MCL1 levels compared with Ki67− NK cells, and this was even more obvious in *Ncr1*[iCre/+]*Bcl2*^{fl/fl} and *Bcl2*[WE/WE] NK cells (Fig. 9 B). These findings suggest that the loss of BCL2 in NK cells results in the preferential survival or selection of NK cells expressing high levels of MCL1, and because dividing NK cells have higher MCL1 levels than noncycling NK cells, the former subset is overrepresented in BCL2-deficient mice. Collectively, these results support a model where MCL1 is indispensable for NK cell survival and BCL2 is critical in noncycling NK cells but redundant when MCL1 expression is elevated during cell cycling. In-

deed, NK cells from mice treated with a strong IL-15 receptor agonist (IL-2/S4B6) present a significant up-regulation of MCL1 to levels similar to that of NK cells from nontreated *Ncr1*[iCre/+]*Bcl2*^{fl/fl} mice (Fig. 9 C). Because both BCL2 and MCL1 were critical for the survival of resting NK cells, we next assessed the role for these two proteins in sequestering the shared BH3-only proapoptotic protein BIM (encoded by *Bcl2l11*). Remarkably, when *Bcl2l11* was deleted at the same time as *Bcl2* in NK cells (*Ncr1*[iCre/+]*Bcl2*^{fl/fl}*Bcl2l11*^{fl/fl}), NK cell development was significantly rescued and similar to that of *Ncr1*[iCre/+] mice (Fig. 9 D). In contrast, deletion of *Bcl2l11* at the same time as *Mcl1* in NK cells (*Ncr1*[iCre/+]*Mcl1*^{fl/fl}-*Bcl2l11*^{fl/fl}) could not rescue NK cell development and was comparable to *Ncr1*[iCre/+]*Mcl1*^{fl/fl} (Fig. 9 D). These data suggest a dominant role for BCL2 in sequestering BIM to prevent NK cell apoptosis but MCL1 is required for sequestering other BH3-only proteins in addition to BIM, presumably
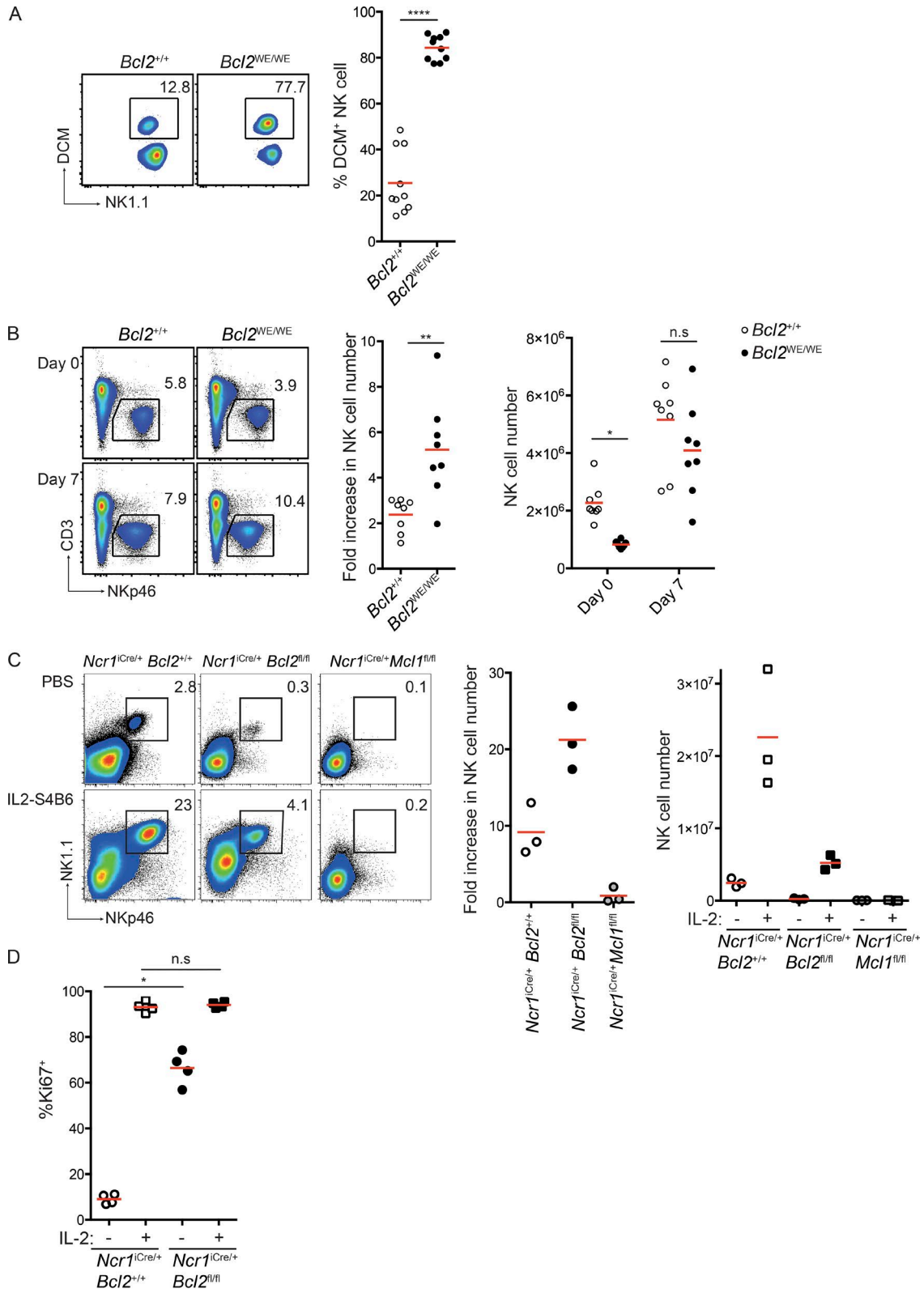
Figure 6. **Impaired NK cell survival in *BCL2*–deficient mice is restored in inflammatory conditions.** (A, left) Representative flow cytometric profiles of *Bcl2*^{+/+} and *Bcl2*[WE/WE] splenic NK cells, stained with dead cell marker (DCM) after 4 h of in vitro culture in complete medium. (right) Percentages of DCM^{+} NK cells (*n* = 21, Mann–Whitney statistical test). (B, left) Representative flow cytometric profiles of spleen NK cells (CD3^{−} NKp46^{+}) from *Bcl2*^{+/+} and *Bcl2*[WE/WE]

NOXA, to protect NK cells from apoptosis. The rescue of BCL2-null NK development by loss of BIM function also resulted in the proportion of Ki67$^+$ NK cells to return to levels similar to control mice, and MCL1 also returned to basal levels (Fig. 9 E). Collectively, these data conclusively demonstrate that loss of BCL2 results in a selection of NK cell in cell cycle because of their high level of MCL1 and that BCL2 does not directly regulate the NK cell cycle.

DISCUSSION

There is a growing interest in developing novel immunotherapies for cancer that increase NK cell frequency, survival, and function. As such, a detailed understanding of the regulators of NK cell homeostasis is essential. Using a forward genetic approach, we have identified a novel mutant mouse ($Bcl2^{WE/WE}$) with a significant reduction in the number of NK cells. The causative mutation was found in the BH4 domain of $Bcl2$. This point mutation did not affect the transcription of the $Bcl2$ gene but resulted in the drastic reduction of BCL2 expression. However, the phenotype of $Bcl2^{WE/WE}$ mice only partially mimicked the phenotype of $Bcl2^{-/-}$ mice (Veis et al., 1993; Nakayama et al., 1994; Bouillet et al., 2001). Like $Bcl2^{-/-}$ mice, $Bcl2^{WE/WE}$ mice presented a severe lymphopenia and a progressive hypopigmentation of the coat. In contrast, $Bcl2^{WE/WE}$ mice did not show growth retardation, short ears, polycystic kidney disease, or premature death. These phenotypic differences suggest that despite our failure to detect BCL2 protein in $Bcl2^{WE/WE}$ hematopoietic cells, some BCL2 protein function remains. The $Bcl2^{WE}$ mutation is thus most likely hypomorphic, with BCL2 stability potentially being compromised by this mutation.

Previous studies have shown that BCL2 plays a critical role in the development of lymphoid progenitor cells from the hematopoietic stem cells (Matsuzaki et al., 1997). To discriminate between the roles of BCL2 in NK cell progenitors and in mature NK cells, BCL2 was genetically deleted in NKp46$^+$ cells using $Ncr1^{iCre/+}Bcl2^{fl/fl}$ mice. This approach allowed us to conclude that the loss of BCL2 function in NK cells severely impacts on their survival and homeostasis. Like MCL1, BCL2 thus has a nonredundant role in NK cell survival in vivo. However, the extent of NK cell lymphopenia in $Ncr1^{iCre/+}Bcl2^{fl/fl}$ mice was less drastic than what we previously reported in $Ncr1^{iCre/+}Mcl1^{fl/fl}$ (Sathe et al., 2014), revealing a hierarchy among BCL2 family members in NK cells where BCL-XL is dispensable, MCL1 is essential, and BCL2 is required for the survival of some but not all NK cells.

The majority of NK cells in the two $Bcl2$ mutant models analyzed in this study were found to be in cell cycle (Ki67$^+$). This phenotype was not caused by a defect in NK cell maturation and overrepresentation of immature NK cells, as the number of NK cells all subsets was significantly reduced in the absence of BCL2 whereas the frequency of cycling cells was significantly increased at all stages of NK cell maturation. This phenotype could be due to an intrinsic role of BCL2 in NK cells or to a bystander effect linked to the partial or profound lymphopenia observed in these mouse models. Knowing that BCL2 protein has a relatively long half-life (Maurer et al., 2006), we observed the presence of a small subset of NKp46$^+$ cells still expressing BCL2 in $Ncr1^{iCre/+}Bcl2^{fl/fl}$ mice. This allowed us to compare the cell cycle phenotype of BCL2$^+$ and BCL2$^-$ NKp46$^+$ subsets present in the same in vivo environment and to demonstrate that the effect of BCL2 on NK cell proliferation was intrinsic and not caused by enhanced homeostatic proliferation. Overexpression of BCL2 has previously been shown to promote the accumulation of B and T lymphocytes in the G0 state, and these BCL2-overexpressing cells in G0 were found to require a longer time to enter the first S phase after mitogenic stimulation compared with control cells in G0 (O'Reilly et al., 1997a,b). Several nonapoptotic functions of BCL2 and other BCL2 family members have been implicated in this phenomenon, including a role for BCL2 in the cell cycle (Janumyan et al., 2003, 2008). A direct role for BCL2 in regulating the NK cell cycle was ruled out by two key findings. First, our analysis of IL-15–stimulated NK cells in response to BCL2 antagonism (ABT-199) in vitro revealed that although a significant increase in the fraction of Ki67$^+$ NK cells was observed after 24 h of ABT-199 treatment, the mean time taken for NK cells to enter their first division was close to 70 h. ABT-199 resulted in a continual loss of NK cells over the 7 d of culture when low IL-15 concentrations were used, whereas NK cell numbers were relatively stable in the vehicle control cultures. At saturating IL-15 concentrations, ABT-199 resulted in clear apoptosis over the first 50 h; however, the proliferation rate of surviving cells was in line with that of vehicle-treated NK cells, and ABT-199–treated cultures demonstrated growth kinetics similar to control NK cells over the remainder of the culture period. These data indicate that BCL2 antagonism directly impacts NK cell survival but not cell division. Last, loss of proapoptotic BIM in BCL2-null NK cell numbers results in their restoration in vivo, and importantly, the relative proportion of Ki67$^+$ NK cells were identical to littermate controls, confirming that the loss of BCL2 does not

mice 0 or 7 d after MCMV infection. (middle) Increase in NK cell number in the spleen 7 d after MCMV infection (n = 8, Mann–Whitney statistical test). (right) Spleen NK cell counts 0 or 7 d after MCMV infection in $Bcl2^{+/+}$ and $Bcl2^{WE/WE}$ mice (n = 8, two-way ANOVA with Bonferroni correction statistical test). (C, left) Representative flow cytometric profiles of spleen NK cells (TCRβ$^-$ NKp46$^+$) from $Ncr1^{iCre/+}Bcl2^{+/+}$, $Ncr1^{iCre/+}Bcl2^{fl/fl}$, and $Ncr1^{iCre/+}Mcl1^{fl/fl}$ mice injected with PBS or IL-2/S4B6. (right) Spleen NK cell fold increase and counts after PBS or IL-2/S4B6 injection. (D) Percentages of Ki67$^+$ NK cells in $Ncr1^{iCre/+}Bcl2^{+/+}$ and $Ncr1^{iCre/+}Bcl2^{fl/fl}$ mice after PBS or IL-2/S4B6 injection. Each dot corresponds to the data obtained for an individual mouse. Horizontal lines indicate the mean. *, P < 0.05; **, P < 0.01; and ****, P < 0.0001.
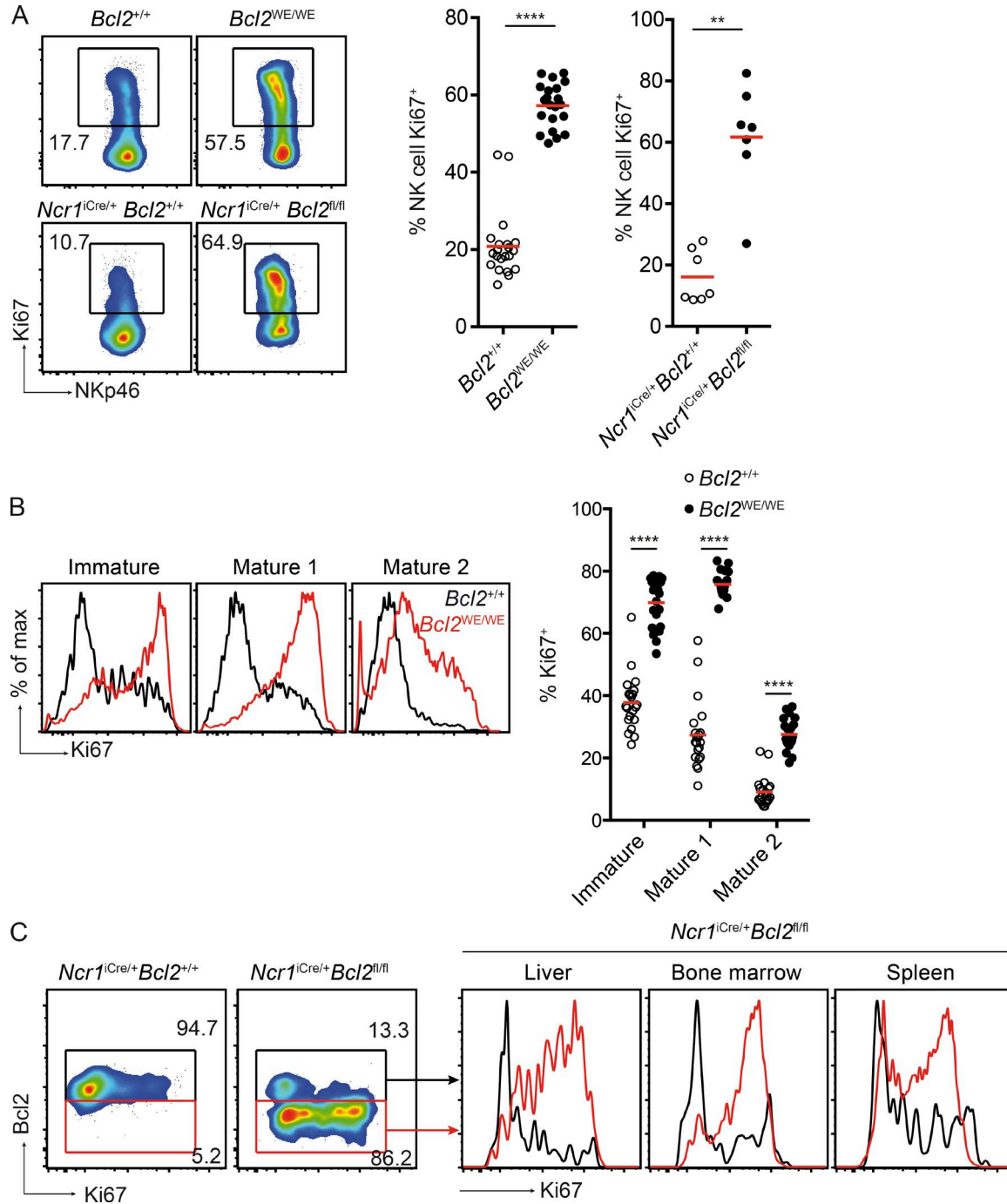
Figure 7. **BCL2 loss is intrinsically linked to an increase of proliferating NK cells.** (A, left) Representative flow cytometric profiles of *Bcl2*^{+/+} and *Bcl2*[WE/WE] or *Ncr1*[iCre/+]*Bcl2*^{+/+} and *Ncr1*[iCre/+]*Bcl2*^{fl/fl} splenic NK cells, stained with anti-Ki67 mAb. (right) Percentages of Ki67^{+} NK cells (*Bcl2*^{+/+}/*Bcl2*[WE/WE] n = 21, *Ncr1*[iCre/+]*Bcl2*^{+/+}/*Ncr1*[iCre/+]*Bcl2*^{fl/fl} n = 7, Mann–Whitney statistical test). Each dot represents the data obtained for a single mouse. (B, left) Representative flow cytometric profiles of Ki67 staining in the indicated NK cell subsets: NK1.1^{+} NKp46^{+} CD27^{+} CD11b^{−} (immature), NK1.1^{+} NKp46^{+} CD27^{+} CD11b^{+} (mature 1), and NK1.1^{+} NKp46^{+} CD27^{−} CD11b^{+} (mature 2). (right) The percentages of Ki67^{+} cells in the indicated NK cell subsets from *Bcl2*^{+/+} and *Bcl2*[WE/WE] mice (n = 21, two-way ANOVA with Bonferroni correction statistical test). Each dot represents the data obtained for a single mouse. (C) Representative flow cytometric profiles of the liver, BM, and spleen NK cells from *Ncr1*[iCre/+]*Bcl2*^{+/+} and *Ncr1*[iCre/+]*Bcl2*^{fl/fl} mice stained with anti-BCL2 and anti-Ki67 mAbs. Data are representative of three independent experiments. Horizontal lines indicate the mean. **, P < 0.01; and ****, P < 0.0001.
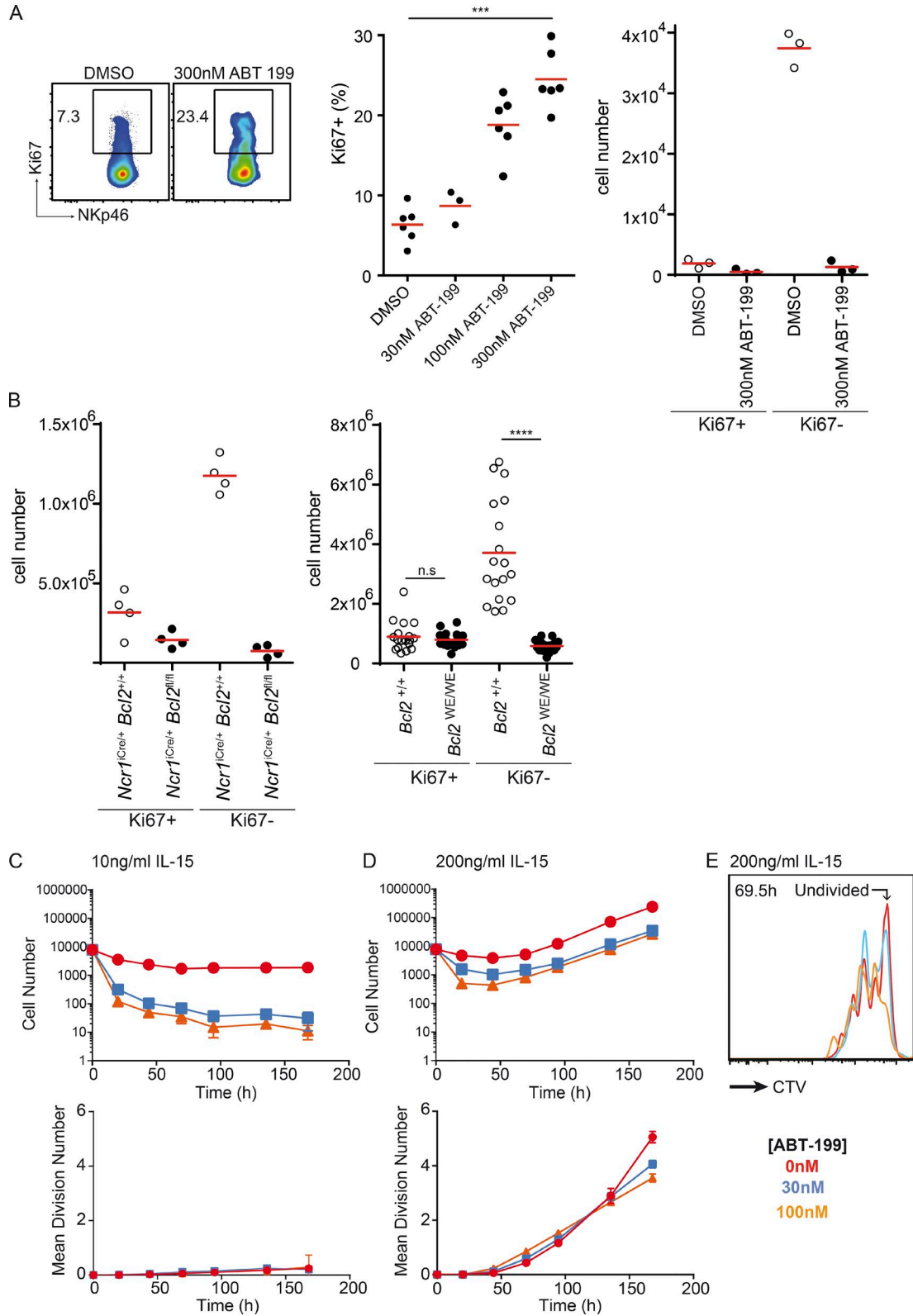
Figure 8. **NK cells in cell cycle are less dependent on BCL2 for their survival.** (A) NK cells from C57BL/6 mice were cultured for 20 h in DMSO or 30 nM, 100 nM, or 300 nM of the BCL2 inhibitor ABT-199. Representative flow cytometric profiles of Ki67 staining on NK cells (left) and percentages of Ki67$^+$ NK cells (middle) are shown (n = 3–6 Kruskal–Wallis statistical test). Ki67$^+$ and Ki67$^-$ NK cell counts are shown for DMSO or 300 nM ABT-199 culture

directly enhance NK cell proliferation. In line with this, it was recently shown that cells rendered deficient for all 16 BCL2 family members proliferate and function normally (O'Neill et al., 2016). We thus propose a model in which BCL2 is required for NK cell survival by antagonizing BIM in nondividing NK cells but is largely redundant when NK cells enter division because of cycling NK cells inherently expressing higher levels of MCL1. The fact that the absolute numbers of Ki67$^+$ NK cells in Bcl2-null and control animals were not significantly different is in accordance with this model.

Interestingly, cycling NK cells do not survive in the absence of MCL1, and reduced levels of MCL1 expression in NK cells ($Ncr1^{iCre/+}Mcl1^{fl/+}$ mice) impair survival at all stages of differentiation and have no effect on the proportion of proliferating (Ki67$^+$) NK cells (Sathe et al., 2014; unpublished data). This indicates that reduced MCL1 expression is equally detrimental to NK cell survival at all stages of the cell cycle. An explanation of why BCL2 loss preferentially affects nonmitotic NK cells may be the posttranslational control of MCL1 protein during mitosis. A previous study reported that although $Mcl1$ mRNA expression did not change during mitotic arrest, MCL1 protein levels declined substantially, and this was dependent on the F-box protein FBW7 and the SCF-type ubiquitin ligase complex, which induced polyubiquitination and degradation (Wertz et al., 2011). Along this line, we observed that in BCL2-sufficient mice, cycling NK cells express higher amount of MCL1 protein than resting NK cells. Moreover, in BCL2-deficient NK cells, MCL1 expression was up-regulated in both subsets and more drastically in the cycling one. Our data indicate that NK cells expressing higher levels of MCL1 are more resistant to apoptosis and are thus enriched in vivo when BCL2 is lost. These results thus support a model where MCL1 is essential and BCL2 being required only in the absence of high MCL1 for NK cell survival. In this model, it is possible that NK cell survival is not only dictated by the net balance between the prosurvival proteins MCL1 and BCL2 but also by functional differences between the two antiapoptotic proteins. Both BCL2 and MCL1 bind and sequester the proapoptotic BH3-only BCL2 family members PUMA and BIM (encoded by $Bcl2l11$), but BCL2 also binds to the BH3-only protein BAD, whereas MCL1 binds to the BH3-only protein NOXA (encoded by $Pmaip1$; Strasser, 2005). These differences in BH3-only protein binding likely explain the differential requirement for BCL2 and MCL1 in vivo, where MCL1 is essential for all NK cell survival and BCL2 is required specifically for noncycling NK cells. In line with this, dual deletion of BIM and MCL1 in NK cells still results in rapid apoptosis and NK cell lymphopenia, suggesting that MCL1 binding to NOXA is critical for the survival of all NK cells. Along these lines, we previously demonstrated that $Pmaip1^{-/-}$ (NOXA-deficient), $Bcl2l11^{-/-}$ (BIM-deficient), and $Bcl2l11^{-/-}Pmaip1^{-/-}$ (BIM/NOXA double-deficient) NK cells all show increasing resistance to apoptosis after IL-15 withdrawal in vitro, whereas $Bad^{-/-}$ NK cells displayed no resistance to apoptosis and $Bim^{-/-}Bad^{-/-}$ NK cells were comparable to $Bim^{-/-}$ NK cells (Huntington et al., 2007a; unpublished data). Thus, the ability of MCL1, but not BCL2, to antagonize NOXA likely accounts for the dominant role of MCL1 in NK cell survival in vivo and explains why loss of BIM only rescues BCL2-null NK cell survival, as NOXA would be antagonized by remaining MCL1.

On a translational front, from the impressive treatment response of CLL patients with B cell malignancies to ABT-199, it appears unlikely that these malignant cells (which are proliferating) are subject to the same preferential expression and dependency on MCL1 during cell cycling (Roberts et al., 2016). Nevertheless, our data suggest that ABT-199 treatment of B cell malignancies that are immunogenic to NK cells might benefit from IL-15 co-treatment to drive high MCL1 levels and protect against ABT-199–induced NK cell apoptosis and loss of the NK cell–mediated antitumor response.
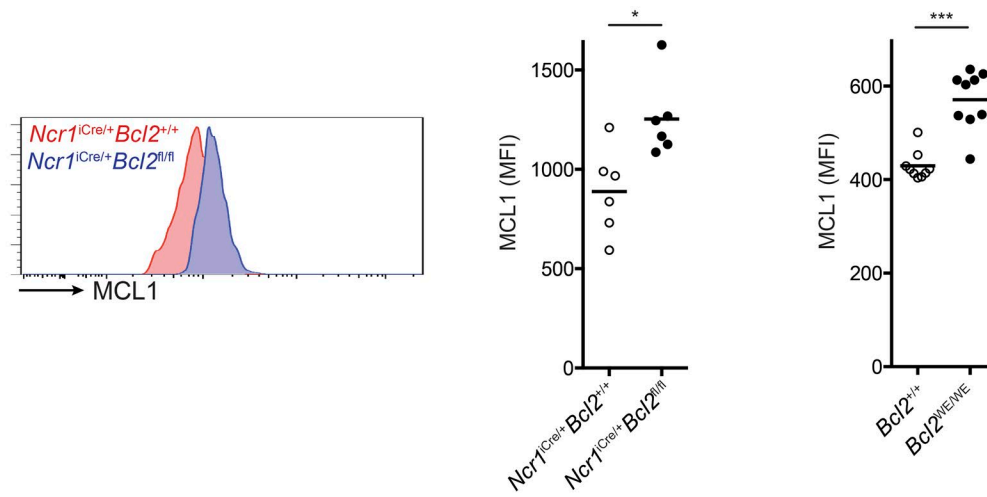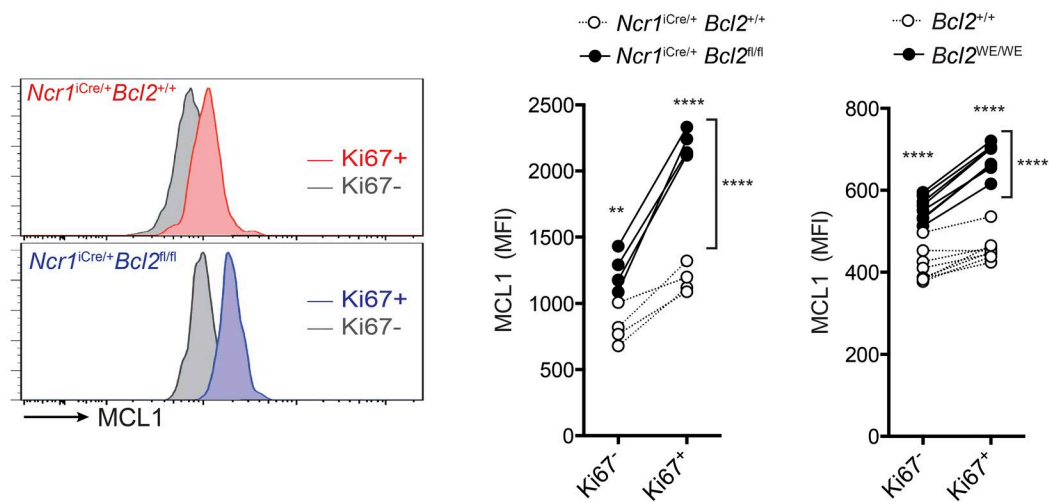
MATERIALS AND METHODS
Mice
WE ($Bcl2^{WE/WE}$) mice were obtained by ENU mutagenesis performed on the C57BL/6J (Charles River) background as described previously (Georgel et al., 2008). Mice were bred and maintained under specific pathogen–free conditions at the Centre d'exploration fonctionnelle Scientifique (CEFOS) in Marseilles and in the Centre d'Immunologie Luminy Marseille. Female and male mice aged 6–12 wk were used for the experiments. All experiments were conducted in accordance with institutional committees and French and European guidelines for animal care. $Bcl2$-loxP (Thorp et al., 2009), $Mcl1$-loxP $Ncr1$-iCre (Sathe et al., 2014), $Bcl2l11$-loxP $Ncr1$-iCre (Delconte et al., 2016b), and $Ncr1$-iCre (Narni-Mancinelli et al., 2011) mice were backcrossed at least 10 times to a C57BL/6 background and were bred and maintained at the Walter and Eliza Hall of Medical Research. All mice were bred and maintained under specific pathogen–free conditions at the Walter and Eliza Hall Institute animal breeding facility, and experiments there were conducted according to the Walter and Eliza Hall Institute (WEHI) and the National Health and Medical Research Council Australia animal ethics guidelines. Both female and male mice aged between 4 and 15 wk were used in this study. All WT controls were either littermates (for ENU) or Bcl2$^{+/+}$Ncr1-iCre$^{KI/+}$ litter-

---

(right). (B) Ki67$^+$ and Ki67$^-$ NK cell counts are shown for $Ncr1^{iCre/+}Bcl2^{+/+}$ and $Ncr1^{iCre/+}Bcl2^{fl/fl}$ mice (left, n = 4) and for $Bcl2^{+/+}$ and $Bcl2^{WE/WE}$ mice (right, n = 19 Kruskal–Wallis statistical test). Horizontal lines indicate the mean. ***, P < 0.001; and ****, P < 0.0001. (C and D) Cell numbers and mean division number versus time graphs of C57BL/6 NK cells cultured in the presence of 10 ng/ml IL-15 (C) or 200 ng/ml IL-15 (D) and 0 nM, 30 nM, or 100 nM of the BCL2 inhibitor ABT-199. Error bars indicate SEM. (E) CTV profiles at 69.5 h, with the undivided peak depicted (n = 1, in triplicate, from pooled spleens of 12 mice).
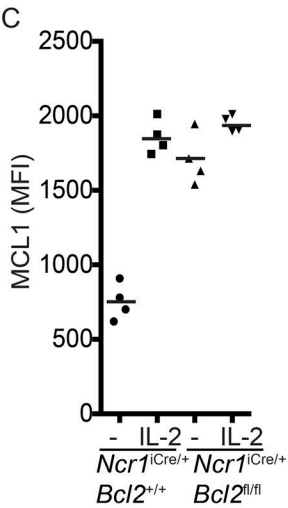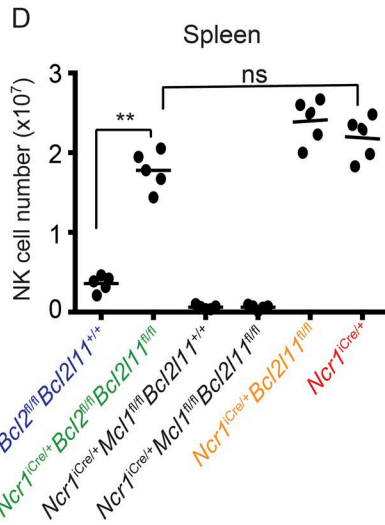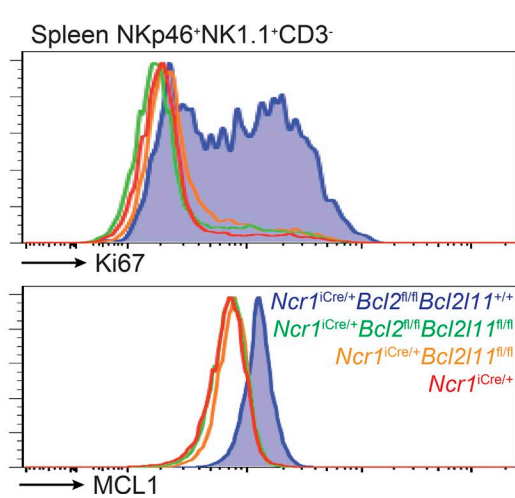
Figure 9. **MCL1 expression is increased in *BCL2*–deficient NK cells.** (A, left) Representative flow cytometric profiles of MCL1 expression in NK cells from *Ncr1*[iCre/+]*Bcl2*^{+/+} and *Ncr1*[iCre/+]*Bcl2*^{fl/fl} are shown. (right) Expression levels of MCL1 (mean fluorescence intensity [MFI]) in NK cells from *Ncr1*[iCre/+]*Bcl2*^{+/+} and *Ncr1*[iCre/+]*Bcl2*^{fl/fl} (*n* = 6), *Bcl2*^{+/+}, and *Bcl2*[WE/WE] mice (*n* = 9, Mann–Whitney statistical test). (B, left) Representative flow cytometric analysis of MCL1 expression in Ki67^{−} and Ki67^{+} NK cells from *Ncr1*[iCre/+]*Bcl2*^{+/+} and *Ncr1*[iCre/+]*Bcl2*^{fl/fl} mice. (right) MCL1 expression (MFI) in cycling (Ki67^{+}) or quiescent (Ki67^{−})

mate controls (for Bcl2$^{fl/fl}$*Ncr1-iCre*$^{KI/+}$). For each model, all mice were housed in the same facility and derived from the same founder colonies.

ENU mutagenesis screen

Mice were bred to produce 30–50 G3 mice per pedigree, a number sufficient to detect concordance between traits of moderate strength and homozygosity at a particular locus, assuming a neutral effect on viability. A single G1 male served as the founder for each pedigree. G3 mice were analyzed to identify an NK cell deficiency. We designed an in vivo screening test allowing the measurement of NK cell cytotoxicity while keeping the mutant mice alive. Splenocytes from *β2m*–knockout and WT mice were labeled with two different concentrations of CFSE (2 or 6 μM, respectively; Thermo Fisher Scientific). Ten million cells of each population were mixed at a 1:1 ratio and injected i.v. into recipient mice (control or G3 mice). 2 d later, mice were anesthetized and 100 μl of blood collected and analyzed by flow cytometry for the presence of CFSE$^+$ donor cells. Percentages of target cell killing were calculated as follows: $100 - ([(\% \beta2m^{-/-} \text{ cells}/\%\text{WT cells}) \text{ output}]/[(\% \beta2m^{-/-} \text{ cells}/\%\text{WT cells}) \text{ input}] \times 100)$.

DNA sequencing

The genetic variations induced by ENU mutagenesis in the *G3-6748* mice from the ENU-148 pedigree were analyzed by whole-exome next-generation sequencing adapted for a SOLiD 5500XL sequencer at the TAGC (Institut National de la Santé et de la Recherche Médicale/Aix-Marseille Université Unité Mixte de Recherche S1090). After whole-exome capture using an Agilent Technologies SureSelect Mouse All Exon kit, short fragments (∼150 nucleotides) from paired-end libraries were prepared with focused acoustic fragmentation (TM S2; Covaris) according to the preparation guide from Thermo Fisher Scientific. Enriched exome fragments were used for the library enrichment according to manufacturer protocol. Templated beads were prepared with the SOLiD EZ Bead System and sequenced according to standard Applied Biosystems and Thermo Fisher Scientific protocols. The sequence reads were first analyzed with the BioScope software suite. Then, variant calling, including small insertions and deletions as well as single-nucleotide variants, was performed with the Genome Variant Analyzer pipeline developed at TAGC.

The seven mutations identified as selectively present in the *WE* mutant were sequenced in six additional ENU-148 mice. DNA extraction from the tails of *WE* and WT mice was performed by phenol/chloroform extraction. For each gene, two primer pairs were designed to detect the fragment amplified by PCR. PCR was performed using a Taq DNA polymerase kit (Promega) and primers targeting Satb2 (5′-CCACAGCACAGGGTTACCTC-3′ [forward] and 5′-AGTAAACCTGAGGGCCATGC-3′ [reverse]; amplicon size 291 pb), Erbb4 (5′-ACCGGTCAGGTTCTTTAATCCA-3′ [forward] and 5′-CTCATCTCAGGTTCTTTAATCCA-3′ [reverse]; amplicon size 469 pb), Arg2 (5′-TGTTGCAGGATGCCACCTAA-3′ [forward] and 5′-TTAGTCTACCCCTGCGCTTG-3′ [reverse]; amplicon size 344 pb), Naip2 (5′-AACTGCTGGATGATGCTGCT-3′ [forward] and 5′-ACCAAAGCTACTTTCCGCCA-3′ [reverse]; amplicon size 392 pb), Slc15a2 (5′-TTGTGACTCACGAGTCTGCC-3′ [forward] and 5′-TCATGCCGTGGTAGCACAAT-3′ [reverse]; amplicon size 452 pb), and Lama1 (5′-TTCAGTCAACTGCCACCTCC-3′ [forward] and 5′-CCAGACGTACTTGCCCTTGT-3′ [reverse]; amplicon size 534 pb).

Cycling conditions were as follows: 94°C for 5 min, 30 cycles of 94°C for 30s, 65°c for 30s, and 72°C for 1 min, with a final extension at 72°C for 5 min, run on a C1000 Thermal Cycler (Bio-Rad Laboratories). Amplification was confirmed using a 2% agarose gel. Then, silica–membrane–based purification of DNA fragments from gels using the QIAquick Gel Extraction kit (QIAGEN) was performed according to the manufacturer's instructions. DNA ranging from 70 pb to 10 kb was purified using a simple and fast bind–wash–elute procedure and an elution volume of 30 μl. Purified DNA samples were subjected to sequence analysis. The sequencing was performed by the international genomic service provider Eurofins Genomics. The whole genomic DNA encoding the *Bcl2* gene of a *WE* mouse was also sequenced.

Quantitative RT–PCR analysis

Total RNA was extracted from splenocytes by using a QIAGEN RNeasy minikit according to the kit manufacturer's instructions. The expression of the *Bcl2* gene and of the three housekeeping genes *Hprt*, *18S*, and *Gapdh* was assessed by quantitative RT-PCR with Applied Biosystems TaqMan Gene expression. Samples were run for 40 cycles on an ABI 7900HT Fast Real-Time PCR System (Applied Biosystems). The relative amount of transcripts for the gene of interest was determined for each sample by normalization with respect to the housekeeping genes, according to the standard ΔCt method. Primers used for *Bcl2* were 5′-GGACTTGAAGTGCCATTGGT-3′ (forward) and 5′-CGGTAGCGACGAGAGAAGTC-3′ (reverse; amplicon size 362 pb).

Mixed–BM chimeric mice

Recipient mice (C57BL/6J CD45.1$^+$) were irradiated twice at 8 Gy. Donor BM cells were obtained from *Bcl2*$^{WE/WE}$ or *Bcl2*$^{+/+}$ mice (both CD45.2$^+$) and mixed at a 1:1 ratio with BM cells of C57BL/6J CD45.1$^+$ mice. Three million cells of each population (ratio of 1:1) were injected i.v. into recipient mice. After 12 wk, spleens were harvested and the percentages of CD45.2$^+$ and CD45.1$^+$ NK cells analyzed by flow cytometry.

Immunoblotting

BCL2 immunoblotting was performed using extracts from splenocytes from *Bcl2*$^{WE/WE}$, *Bcl2*$^{WE/+}$, and *Bcl2*$^{+/+}$ mice. Splenocytes were lysed with a lysis buffer (25 mM Hepes, 150 mM NaCl, 1% NP-40, 10 mM MgCl$_2$, 1 mM EDTA, 2% glycerol, and protease inhibitor cocktail tablets; Roche). Protein assays were performed with a BCA kit (Thermo Fisher Scientific). Then, 100 µg protein per sample in LDS sample buffer (Invitrogen) was run in a 4–12% Bis-Tris precast electrophoresis gel in MES SDS running buffer (Invitrogen). Proteins were then transferred onto a nitrocellulose membrane using the iBlot Dry blotting system (Thermo Fisher Scientific). Membranes were saturated by incubation for 1 h with 0.5% Tween 20, 5% milk in PBS, stained with antibodies against BCL2 (10C4; Santa Cruz Biotechnology, Inc.), and then incubated with an anti–mouse IgG-HRP Easy Blot secondary antibody (Gene Tex). Antibody binding was revealed with an ECL kit (GE Healthcare). After stripping of the membranes, staining for β-actin (AC-15; Sigma-Aldrich) was performed using the same protocol (loading control).

Cell preparation and in vitro treatment

Splenocyte suspensions were obtained by mechanical disruption of mouse spleen. Red blood cells were then lysed using RBC lysis solution (eBioscience). Splenocytes were used for flow cytometry and Western blot analyses. In some experiments, splenocytes were incubated for 4 h in vitro in complete medium or for 20 h with 10 ng/ml IL-15 and ABT-199 (Souers et al., 2013) or DMSO (vehicle control). NK cells enriched with the NK Cell Isolation kit II (Miltenyi Biotec) were cultured 7 d with 5,000 U/ml IL-2 (Chiron) to obtain LAK cells. NK cells or LAK cells were also activated in 96-well plates coated with 30 µg/ml anti–NK1.1 (eBioscience) with the cytokines, 25 ng/ml IL-12 (eBioscience) and 20 ng/ml IL-18 (MBL), with 200 ng/ml PMA plus 1 µg/ml ionomycin or with of YAC-1 cells at a 1:1 ratio, in the presence of monensin and brefeldin A (1:1,000 GolgiPlug and 1:1,500 GolgiStop; BD) in complete medium for 4 h at 37°C.

BM cells were obtained by flushing femurs and tibias, and red blood cells were lysed using RBC lysis solution (eBioscience). For the analysis of liver lymphocytes, mice were anesthetized and immediately perfused with PBS before the collection of the organs. Livers were then mechanically disrupted in PBS in a cell strainer, and the cell suspensions were washed three times with PBS. Samples were

then enriched for lymphocytes by centrifugation on a Percoll gradient (GE Healthcare). Blood was collected under anesthesia and transferred into Trucount tubes (BD) for enumeration by flow cytometry.

E0771 tumor rejection

E0771.LMB mCherry+ tumor metastasis models were performed as previously described (Delconte et al., 2016a). In brief, 5×10^5 E0771.LMB mCherry+ tumor cells were injected i.v. into the tail vein of the indicated strains of mice. Lungs were harvested 14 d later and metastatic burden quantified by imaging ex vivo using an IVIS Lumina XR-III (Caliper Life Sciences) or by duplex quantitative PCR for expression of mCherry relative to vimentin, as described previously (Rautela et al., 2015).

Flow cytometric analysis

Flow cytometric analysis was performed on an LSR II (four-laser blue/red/violet/UV flow cytometry analyzer; BD) or FACSVerse (three-laser blue/red/violet flow cytometry analyzer; BD). Antibodies used included BCL2-PE (10C4, 1/100), NKp46–PreCP (29A1.4, 1/100), NKp46-FITC (29A1.4, 1/100), CD49d-PE (DX5, 1/400), CD49a-APC (Ha31/8, 1/400), CD27-PE (LG.3A10, 1/100), CD27-PreCP (LG.3A10, 1/200), CD11b-V450 (M1/70, 1/600), KLRG1-APC (2F1, 1/400), CD43-FITC (S7, 1/100), CD107a-FITC (1D4B, 1/50), IFN-γ-A647 (XMG1.2, 1/200), NK1.1-APC (PK136, 1/400), NK1.1-PC7 (PK136, 1/400), CD3-V500 (500A2, 1/150), CD19-APC-Cy7 (1D3, 1/200), CD19-FITC (1D3, 1/800), CD45.1-PE-Cy7 (A20, 1/200), CD45.2-A700 (104, 1/400), and Ki67 (B56, 1/50). These reagents were obtained from eBioscience, BioLegend, and BD, and LIVE/DEAD Fixable Dead Cell Stain was from Molecular Probes. Anti-MCL1 antibody was generated at the WEHI monoclonal antibody laboratory (Bundoora, Australia; Okamoto et al., 2014).

IL–2/S4B6 treatment and MCMV infection

For IL-2 treatment, 1.5 µg IL-2 (PeproTech) and 10 µg anti–IL-2 mAb (S4B6) were incubated together at 37°C for 30 min and then injected i.p. as previously described (Holmes et al., 2014). For MCMV infection, mice matched in sex and age were infected by i.p. injection with 100 pfu/g of the Smith strain of MCMV virus. Cell proliferation was analyzed on days 0 and 7 after the injection.

In vitro NK cell dynamics and modeling

Mouse NK lymphocytes were harvested from spleens of C57BL/6 mice. A single-cell suspension was prepared by forcing spleens through 70-µM sieves, and NK cells were isolated using the EasySep Mouse NK cell Isolation kit (STEMCELL Technologies) according to manufacturer's specifications. Enrichment of NK cells was confirmed by flow cytometry with a yield of 87% NK lymphocytes. NK cells were incubated with 5 µM CTV (Thermo Fisher Scientific) according to

manufacturer's instructions, and 8×10^3 labeled cells were seeded into 96-well round bottom plates in Iscove's modified Dulbecco's medium containing titrated concentrations of IL-15 (0, 3.16, 10, 31.6, 100, and 200 ng/ml) and ABT-199 (0, 30, and 100 nM). Cells were incubated in a humidified environment at 37°C containing 5% CO_2 for 10 d and analyzed by flow cytometry at routine time points on a BD FACS Canto.

NK cell survival and mean division numbers were determined using the precursor cohort–based method (Hawkins et al., 2007; Marchingo et al., 2014).

Statistical analysis

Statistical analyses were performed using Prism 5 (Graph-Pad Software). Kruskal–Wallis, Mann–Whitney, and two-way ANOVA tests with Bonferroni correction were used as indicated in the figure legends. Significance is indicated as follows: *, $P < 0.05$; **, $P < 0.01$; ***, $P < 0.001$; and ****, $P < 0.0001$.

REFERENCES

Armant, M., G. Delespesse, and M. Sarfati. 1995. IL-2 and IL-7 but not IL-12 protect natural killer cells from death by apoptosis and up-regulate bcl-2 expression. *Immunology.* 85:331–337.

Bergamaschi, C., J. Bear, M. Rosati, R.K. Beach, C. Alicea, R. Sowder, E. Chertova, S.A. Rosenberg, B.K. Felber, and G.N. Pavlakis. 2012. Circulating IL-15 exists as heterodimeric complex with soluble IL-15Rα in human and mouse serum. *Blood.* 120:e1–e8. http://dx.doi.org/10.1182/blood-2011-10-384362

Bouillet, P., S. Cory, L.C. Zhang, A. Strasser, and J.M. Adams. 2001. Degenerative disorders caused by Bcl-2 deficiency prevented by loss of its BH3-only antagonist Bim. *Dev. Cell.* 1:645–653. http://dx.doi.org/10.1016/S1534-5807(01)00083-1

Boyman, O., M. Kovar, M.P. Rubinstein, C.D. Surh, and J. Sprent. 2006. Selective stimulation of T cell subsets with antibody-cytokine immune complexes. *Science.* 311:1924–1927. http://dx.doi.org/10.1126/science.1122927

Burkett, P.R., R. Koka, M. Chien, S. Chai, D.L. Boone, and A. Ma. 2004. Coordinate expression and trans presentation of interleukin (IL)-15Ralpha and IL-15 supports natural killer cell and memory CD8+ T cell homeostasis. *J. Exp. Med.* 200:825–834. http://dx.doi.org/10.1084/jem.20041389

Cooper, M.A., J.E. Bush, T.A. Fehniger, J.B. VanDeusen, R.E. Waite, Y. Liu, H.L. Aguila, and M.A. Caligiuri. 2002. In vivo evidence for a dependence on interleukin 15 for survival of natural killer cells. *Blood.* 100:3633–3638. http://dx.doi.org/10.1182/blood-2001-12-0293

Delconte, R.B., T.B. Kolesnik, L.F. Dagley, J. Rautela, W. Shi, E.M. Putz, K. Stannard, J.G. Zhang, C. Teh, M. Firth, et al. 2016a. CIS is a potent checkpoint in NK cell–mediated tumor immunity. *Nat. Immunol.* 17:816–824. http://dx.doi.org/10.1038/ni.3470

Delconte, R.B., W. Shi, P. Sathe, T. Ushiki, C. Seillet, M. Minnich, T.B. Kolesnik, L.C. Rankin, L.A. Mielke, J.G. Zhang, et al. 2016b. The helix-loop-helix protein ID2 governs NK cell fate by tuning their sensitivity to interleukin-15. *Immunity.* 44:103–115. http://dx.doi.org/10.1016/j.immuni.2015.12.007

Dubois, S., J. Mariner, T.A. Waldmann, and Y. Tagaya. 2002. IL-15Ralpha recycles and presents IL-15 In trans to neighboring cells. *Immunity.* 17:537–547. http://dx.doi.org/10.1016/S1074-7613(02)00429-6

Georgel, P., X. Du, K. Hoebe, and B. Beutler. 2008. ENU mutagenesis in mice. *Methods Mol. Biol.* 415:1–16.

Hawkins, E.D., M. Hommel, M.L. Turner, F.L. Battye, J.F. Markham, and P.D. Hodgkin. 2007. Measuring lymphocyte proliferation, survival and differentiation using CFSE time-series data. *Nat. Protoc.* 2:2057–2067. http://dx.doi.org/10.1038/nprot.2007.297

Hodge, D.L., J. Yang, M.D. Buschman, P.M. Schaughency, H. Dang, W. Bere, Y. Yang, R. Savan, J.J. Subleski, X.M. Yin, et al. 2009. Interleukin-15 enhances proteasomal degradation of bid in normal lymphocytes: implications for large granular lymphocyte leukemias. *Cancer Res.* 69:3986–3994. http://dx.doi.org/10.1158/0008-5472.CAN-08-3735

Holmes, M.L., N.D. Huntington, R.P. Thong, J. Brady, Y. Hayakawa, C.E. Andoniou, P. Fleming, W. Shi, G.K. Smyth, M.A. Degli-Esposti, et al. 2014. Peripheral natural killer cell maturation depends on the transcription factor Aiolos. *EMBO J.* 33:2721–2734. http://dx.doi.org/10.15252/embj.201487900

Huntington, N.D. 2014. The unconventional expression of IL-15 and its role in NK cell homeostasis. *Immunol. Cell Biol.* 92:210–213. http://dx.doi.org/10.1038/icb.2014.1

Huntington, N.D., H. Puthalakath, P. Gunn, E. Naik, E.M. Michalak, M.J. Smyth, H. Tabarias, M.A. Degli-Esposti, G. Dewson, S.N. Willis, et al. 2007a. Interleukin 15-mediated survival of natural killer cells is determined by interactions among Bim, Noxa and Mcl-1. *Nat. Immunol.* 8:856–863. http://dx.doi.org/10.1038/ni1487

Huntington, N.D., H. Tabarias, K. Fairfax, J. Brady, Y. Hayakawa, M.A. Degli-Esposti, M.J. Smyth, D.M. Tarlinton, and S.L. Nutt. 2007b. NK cell maturation and peripheral homeostasis is associated with KLRG1 up-regulation. *J. Immunol.* 178:4764–4770. http://dx.doi.org/10.4049/jimmunol.178.8.4764

Huntington, N.D., C.A. Vosshenrich, and J.P. Di Santo. 2007c. Developmental pathways that generate natural-killer-cell diversity in mice and humans. *Nat. Rev. Immunol.* 7:703–714. http://dx.doi.org/10.1038/nri2154

Huntington, N.D., N. Legrand, N.L. Alves, B. Jaron, K. Weijer, A. Plet, E. Corcuff, E. Mortier, Y. Jacques, H. Spits, and J.P. Di Santo. 2009. IL-15 trans-presentation promotes human NK cell development and differentiation in vivo. *J. Exp. Med.* 206:25–34. http://dx.doi.org/10.1084/jem.20082013

Jaeger, B.N., J. Donadieu, C. Cognet, C. Bernat, D. Ordoñez-Rueda, V. Barlogis, N. Mahlaoui, A. Fenis, E. Narni-Mancinelli, B. Beaupain, et al. 2012. Neutrophil depletion impairs natural killer cell maturation, function, and homeostasis. *J. Exp. Med.* 209:565–580. http://dx.doi.org/10.1084/jem.20111908

Janumyan, Y.M., C.G. Sansam, A. Chattopadhyay, N. Cheng, E.L. Soucie, L.Z. Penn, D. Andrews, C.M. Knudson, and E. Yang. 2003. Bcl-xL/Bcl-2 coordinately regulates apoptosis, cell cycle arrest and cell cycle entry. *EMBO J.* 22:5459–5470. http://dx.doi.org/10.1093/emboj/cdg533

Janumyan, Y., Q. Cui, L. Yan, C.G. Sansam, M. Valentin, and E. Yang. 2008. G0 function of BCL2 and BCL-xL requires BAX, BAK, and p27 phosphorylation by Mirk, revealing a novel role of BAX and BAK in quiescence regulation. *J. Biol. Chem.* 283:34108–34120. http://dx.doi.org/10.1074/jbc.M806294200

Jiang, S., R. Munker, and M. Andreeff. 1996. Bcl-2 is expressed in human natural killer cells and is regulated by interleukin-2. *Nat. Immun.* 15:312–317.

Koka, R., P.R. Burkett, M. Chien, S. Chai, F. Chan, J.P. Lodolce, D.L. Boone, and A. Ma. 2003. Interleukin (IL)-15R[alpha]–deficient natural killer cells survive in normal but not IL-15R[alpha]–deficient mice. *J. Exp. Med.* 197:977–984. http://dx.doi.org/10.1084/jem.20021836

Lucas, M., W. Schachterle, K. Oberle, P. Aichele, and A. Diefenbach. 2007. Dendritic cells prime natural killer cells by trans-presenting interleukin 15. *Immunity.* 26:503–517. http://dx.doi.org/10.1016/j.immuni.2007.03.006

Lucas, M., C. Vonarbourg, P. Aichele, and A. Diefenbach. 2010. Studying NK cell/dendritic cell interactions. *Methods Mol. Biol.* 612:97–126. http://dx.doi.org/10.1007/978-1-60761-362-6_8

Marchingo, J.M., A. Kan, R.M. Sutherland, K.R. Duffy, C.J. Wellard, G.T. Belz, A.M. Lew, M.R. Dowling, S. Heinzel, and P.D. Hodgkin. 2014. T cell signaling. Antigen affinity, costimulation, and cytokine inputs sum linearly to amplify T cell expansion. *Science.* 346:1123–1127. http://dx.doi.org/10.1126/science.1260044

Matsuzaki, Y., K. Nakayama, K. Nakayama, T. Tomita, M. Isoda, D.Y. Loh, and H. Nakauchi. 1997. Role of bcl-2 in the development of lymphoid cells from the hematopoietic stem cell. *Blood.* 89:853–862.

Maurer, U., C. Charvet, A.S. Wagman, E. Dejardin, and D.R. Green. 2006. Glycogen synthase kinase-3 regulates mitochondrial outer membrane permeabilization and apoptosis by destabilization of MCL-1. *Mol. Cell.* 21:749–760. http://dx.doi.org/10.1016/j.molcel.2006.02.009

Mortier, E., T. Woo, R. Advincula, S. Gozalo, and A. Ma. 2008. IL-15Ralpha chaperones IL-15 to stable dendritic cell membrane complexes that activate NK cells via trans presentation. *J. Exp. Med.* 205:1213–1225. http://dx.doi.org/10.1084/jem.20071913

Nakayama, K., K. Nakayama, I. Negishi, K. Kuida, H. Sawa, and D.Y. Loh. 1994. Targeted disruption of Bcl-2 alpha beta in mice: occurrence of gray hair, polycystic kidney disease, and lymphocytopenia. *Proc. Natl. Acad. Sci. USA.* 91:3700–3704. http://dx.doi.org/10.1073/pnas.91.9.3700

Narni-Mancinelli, E., J. Chaix, A. Fenis, Y.M. Kerdiles, N. Yessaad, A. Reynders, C. Gregoire, H. Luche, S. Ugolini, E. Tomasello, et al. 2011. Fate mapping analysis of lymphoid cells expressing the NKp46 cell surface receptor. *Proc. Natl. Acad. Sci. USA.* 108:18324–18329. http://dx.doi.org/10.1073/pnas.1112064108

Narni-Mancinelli, E., B.N. Jaeger, C. Bernat, A. Fenis, S. Kung, A. De Gassart, S. Mahmood, M. Gut, S.C. Heath, J. Estellé, et al. 2012. Tuning of natural killer cell reactivity by NKp46 and Helios calibrates T cell responses. *Science.* 335:344–348. http://dx.doi.org/10.1126/science.1215621

O'Neill, K.L., K. Huang, J. Zhang, Y. Chen, and X. Luo. 2016. Inactivation of prosurvival Bcl-2 proteins activates Bax/Bak through the outer mitochondrial membrane. *Genes Dev.* 30:973–988. http://dx.doi.org/10.1101/gad.276725.115

O'Reilly, L.A., A.W. Harris, and A. Strasser. 1997a. bcl-2 transgene expression promotes survival and reduces proliferation of CD3-CD4-CD8- T cell progenitors. *Int. Immunol.* 9:1291–1301. http://dx.doi.org/10.1093/intimm/9.9.1291

O'Reilly, L.A., A.W. Harris, D.M. Tarlinton, L.M. Corcoran, and A. Strasser. 1997b. Expression of a bcl-2 transgene reduces proliferation and slows turnover of developing B lymphocytes in vivo. *J. Immunol.* 159:2301–2311.

Okamoto, T., L. Coultas, D. Metcalf, M.F. van Delft, S.P. Glaser, M. Takiguchi, A. Strasser, P. Bouillet, J.M. Adams, and D.C. Huang. 2014. Enhanced stability of Mcl1, a prosurvival Bcl2 relative, blunts stress-induced apoptosis, causes male sterility, and promotes tumorigenesis. *Proc. Natl. Acad. Sci. USA.* 111:261–266. http://dx.doi.org/10.1073/pnas.1321259110

Ranson, T., C.A. Vosshenrich, E. Corcuff, O. Richard, W. Müller, and J.P. Di Santo. 2003. IL-15 is an essential mediator of peripheral NK-cell homeostasis. *Blood.* 101:4887–4893. http://dx.doi.org/10.1182/blood-2002-11-3392

Rautela, J., N. Baschuk, C.Y. Slaney, K.M. Jayatilleke, K. Xiao, B.N. Bidwell, E.C. Lucas, E.D. Hawkins, P. Lock, C.S. Wong, et al. 2015. Loss of host type-I IFN signaling accelerates metastasis and impairs NK-cell antitumor function in multiple models of breast cancer. *Cancer Immunol. Res.* 3:1207–1217. http://dx.doi.org/10.1158/2326-6066.CIR-15-0065

Roberts, A.W., M.S. Davids, J.M. Pagel, B.S. Kahl, S.D. Puvvada, J.F. Gerecitano, T.J. Kipps, M.A. Anderson, J.R. Brown, L. Gressick, et al. 2016. Targeting BCL2 with Venetoclax in relapsed chronic lymphocytic leukemia. *N. Engl. J. Med.* 374:311–322. http://dx.doi.org/10.1056/NEJMoa1513257

Rubinstein, M.P., M. Kovar, J.F. Purton, J.H. Cho, O. Boyman, C.D. Surh, and J. Sprent. 2006. Converting IL-15 to a superagonist by binding to soluble IL-15Ralpha. *Proc. Natl. Acad. Sci. USA.* 103:9166–9171. http://dx.doi.org/10.1073/pnas.0600240103

Rybner-Barnier, C., C. Jacquemot, C. Cuche, G. Doré, L. Majlessi, M.M. Gabellec, A. Moris, O. Schwartz, J. Di Santo, A. Cumano, et al. 2006. Processing of the bovine spongiform encephalopathy-specific prion protein by dendritic cells. *J. Virol.* 80:4656–4663. http://dx.doi.org/10.1128/JVI.80.10.4656-4663.2006

Sandau, M.M., K.S. Schluns, L. Lefrancois, and S.C. Jameson. 2004. Cutting edge: Transpresentation of IL-15 by bone marrow-derived cells necessitates expression of IL-15 and IL-15R alpha by the same cells. *J. Immunol.* 173:6537–6541. http://dx.doi.org/10.4049/jimmunol.173.11.6537

Sathe, P., R.B. Delconte, F. Souza-Fonseca-Guimaraes, C. Seillet, M. Chopin, C.J. Vandenberg, L.C. Rankin, L.A. Mielke, I. Vikstrom, T.B. Kolesnik, et al. 2014. Innate immunodeficiency following genetic ablation of Mcl1 in natural killer cells. *Nat. Commun.* 5:4539. http://dx.doi.org/10.1038/ncomms5539

Soldaini, E., S. John, S. Moro, J. Bollenbacher, U. Schindler, and W.J. Leonard. 2000. DNA binding site selection of dimeric and tetrameric Stat5 proteins reveals a large repertoire of divergent tetrameric Stat5a binding sites. *Mol. Cell. Biol.* 20:389–401. http://dx.doi.org/10.1128/MCB.20.1.389-401.2000

Souers, A.J., J.D. Leverson, E.R. Boghaert, S.L. Ackler, N.D. Catron, J. Chen, B.D. Dayton, H. Ding, S.H. Enschede, W.J. Fairbrother, et al. 2013. ABT-199, a potent and selective BCL-2 inhibitor, achieves antitumor activity while sparing platelets. *Nat. Med.* 19:202–208. http://dx.doi.org/10.1038/nm.3048

Strasser, A. 2005. The role of BH3-only proteins in the immune system. *Nat. Rev. Immunol.* 5:189–200. http://dx.doi.org/10.1038/nri1568

Thorp, E., Y. Li, L. Bao, P.M. Yao, G. Kuriakose, J. Rong, E.A. Fisher, and I. Tabas. 2009. Brief report: increased apoptosis in advanced atherosclerotic lesions of Apoe$^{-/-}$ mice lacking macrophage Bcl-2. *Arterioscler. Thromb. Vasc. Biol.* 29:169–172. http://dx.doi.org/10.1161/ATVBAHA.108.176495

Veis, D.J., C.M. Sorenson, J.R. Shutter, and S.J. Korsmeyer. 1993. Bcl-2-deficient mice demonstrate fulminant lymphoid apoptosis, polycystic kidneys, and hypopigmented hair. *Cell.* 75:229–240. http://dx.doi.org/10.1016/0092-8674(93)80065-M

Wertz, I.E., S. Kusam, C. Lam, T. Okamoto, W. Sandoval, D.J. Anderson, E. Helgason, J.A. Ernst, M. Eby, J. Liu, et al. 2011. Sensitivity to antitubulin chemotherapeutics is regulated by MCL1 and FBW7. *Nature.* 471:110–114. http://dx.doi.org/10.1038/nature09779

Zheng, X., Y. Wang, H. Wei, B. Ling, R. Sun, and Z. Tian. 2008. Bcl-xL is associated with the anti-apoptotic effect of IL-15 on the survival of CD56(dim) natural killer cells. *Mol. Immunol.* 45:2559–2569. http://dx.doi.org/10.1016/j.molimm.2008.01.001